A Micromechanical Investigation of Interfacial Transport Processes. I. Interfacial Conservation Equations

Gretchen M. Mavrovouniotis and Howard Brenner

| **Email alerting service** | Receive free email alerts when new articles cite this article - sign up in the box at the top right-hand corner of the article or click **here** |

A micromechanical investigation of interfacial transport processes. I. Interfacial conservation equations

By Gretchen M. Mavrovouniotis† and Howard Brenner

Department of Chemical Engineering, Massachusetts Institute of Technology, Cambridge, Massachusetts 02139, U.S.A.

Contents

Macroscale interfacial conservation equations are derived for transport processes occurring in immiscible fluid–fluid systems possessing moving and deforming interfaces via a rigorous matched asymptotic expansion scheme from the more exact, continuous ('diffuse') microscale equations underlying them. A surface-fixed

Phil. Trans. R. Soc. Lond. A (1993) **345**, 165–207

Printed in Great Britain

165

© 1993 The Royal Society

Vol. 345. A (15 November 1993)

coordinate system is developed for the parameterization of the interface, alleviating approximations which result when either a material or a space-fixed control volume is used to investigate systems undergoing interphase mass transfer.

1. Introduction

Interfacial systems have traditionally been viewed (Scriven 1960, see the extended derivation in Aris 1962; Slattery 1964*a*, *b*; Ghez 1966; Moeckel 1975; Slattery 1980; Waxman 1984; Gurtin & Struthers 1990) as consisting of two (or more) immiscible 'homogeneous' bulk fluids separated by a singular two-dimensional surface. The two bulk fluids are each separately characterized by bulk material properties which, though separately continuous within each of the two bulk-fluid regions, may suffer jump discontinuities across the interface. The two-dimensional surface composing the interface is itself characterized as being endowed with distinct interfacial material properties of its own, such as interfacial tension in the static case and interfacial shear and dilatational viscosities in the dynamic case. Conservation and constitutive equations are separately written for the two bulk fluids and the dividing surface. The transport equations for the two-dimensional surface then play the role of boundary conditions for the bulk equations, furnishing the so-called jump boundary conditions imposed upon the generally discontinuous bulk-fluid fields across the singular surface. Although the above view of the interface is quite useful for examining material interfaces, it is inherently ambiguous when mass transfer occurs across the interface. In particular, how are *material* interfacial properties to be assigned to the two-dimensional interface when the latter is not composed of material points?

The two-dimensional, 'macroscale' view of the interface is, however, universally recognized as only a useful approximation of the true physical state of the system (Gibbs 1957). In actuality, the interfacial region between the two immiscible fluids is a highly inhomogeneous, three-dimensional transition region over which rapid changes in material properties (and the corresponding fields, such as mass density, species concentration, stress, etc.) may occur. In this diffuse, three-dimensional, 'microscale' view, the relevant continuum fields are assumed to vary continuously throughout the entire space, albeit some fields extremely steeply within the interfacial region in the direction of the surface normal.

Such a microscale conception of the interface has previously been used (Eliassen 1963; Murphy 1966; Slattery 1967; Deemer & Slattery 1978; Goodrich 1981; Alts & Hutter 1988) to theoretically investigate the transport properties of moving and deforming interfaces. In these investigations, an important distinction is made between the 'true', continuous, three-dimensional (microscale) view of the interfacial region and the useful, but approximate, discontinuous, two-dimensional (macroscale) view of the interface. The macroscale view of the interface is, in such 'classical' theories, reconciled with the microscale view via the choice of a Gibbs dividing surface (Gibbs 1957; Tolman 1948; Buff 1956; Ono & Kondo 1960). All of the macroscale inhomogeneities arising from the three-dimensional character of the interfacial region are 'lumped' into so-called surface-excess and related interfacial fields assigned at each point of the two-dimensional interface. These theories generally attempt to construct an *equivalent* two-dimensional, macroscale model of the interface. However, by attempting to furnish an exact reconciliation of the
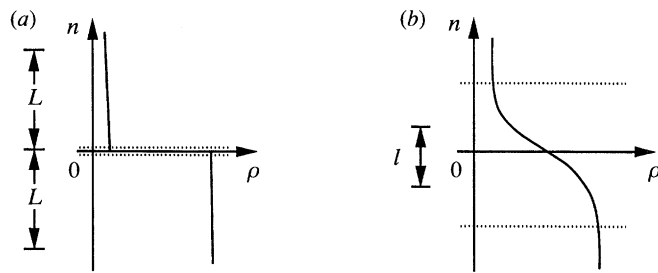
Figure 1. Macroscale (L) against microscale (l) views of the same field: an example. Variation in the fluid mass density ρ as a function of the normal distance n above the interface: (*a*) traditional, macroscale view, displaying a discontinuous density change at the interface $n = 0$; (*b*) microscale view, showing an expanded scale for the diffuse interfacial region.

micro- and macroscale views, this approach ignores the inherently *asymptotic* nature of the macroscale view, which only approximates – but cannot exactly reproduce – the detailed physics of the original microscale problem.

The microscale view of the interface can be quite useful for examining the problem of interphase mass transport. Slattery (1967), recognizing that previous macroscale approaches (Scriven 1960; Slattery 1964*a*, *b*) for investigating interfacial mass transport were deficient in that 'the concept of following a region of material within the interface contradicts the assumption of simultaneous interphase mass transfer', used the microscale view of the interface to examine interphase mass transport. This work was later extended and clarified by Deemer & Slattery (1978). More recently, Dell'Isola & Romano (1987*a*, *b*) also examined this problem. Rather than assigning surface-*excess* properties to the interface, they treated the interface as a film through which mass could be transported and whose thickness approaches zero.

An asymptotic scheme for systematically deriving the macroscale interfacial conservation and constitutive equations from knowledge of the comparable microscale equations was developed by Brenner (1979) for static interfacial systems and by Brenner & Leal (1977, 1978*a*, *b*, 1982) for systems containing adsorbed surfactant species undergoing surface diffusion and convection as well as mass transport across the interface. Matched asymptotic expansion techniques provided a rational method for systematically reconciling the macro- and microscale views.

In this paper, the latter asymptotic approaches are generalized and extended to include systems containing moving and deforming interfaces. To better understand the asymptotic approach presented herein, consider a system consisting of two fluids whose common 'boundary' is a thin three-dimensional transition region. Let the characteristic length l of the microscale be chosen as the effective 'thickness' of this interfacial transition region. Imagine an experimental probe able to discern field changes occurring over the small length scale l, while still sampling a sufficiently large region of space (and time) to permit the random motions of individual molecules to average out and, hence, enabling the system to be treated as a continuum. (This assumption limits the applicability of the subsequent theory to circumstances for which a continuum description of the diffuse interfacial region is valid.) Use of this 'microscale probe' permits the mapping of each continuum field of the system throughout the entire fluid space. Each such field, when observed from the microscale, is assumed to be strictly continuous throughout the entire space, including the interfacial transition region (for example, see figure 1*b*).

Suppose the size of the probe is incrementally increased, permitting the probe to

7-2

sample ever larger fluid regions. At some stage, the probe will clearly become too coarse to detect any rapid changes occurring over the length scale l of the interfacial transition region, although its aperture will still be sufficiently small to detect and record those more gradual field changes occurring within the separate 'bulk-fluid' regions. Define the characteristic length L of the macroscale to be the minimum length scale over which such a probe can detect changes in the continuum fields. Since this 'macroscale probe' is, by definition, able only to discern continuum field changes occurring over the larger length scale L characteristic of changes within the bulk-fluid regions, the interfacial region appears to be a singular two-dimensional surface to the 'macroscale observer' employing the probe. Using this macroscale probe, a systematic mapping of any physical continuum field of the system can be performed throughout the entire space. Although all relevant physical fields appear separately continuous within each of the two bulk-fluid regions, they may appear (to the macroscale observer) to change discontinuously upon crossing the interface (for example, see figure 1a).

As l is generally of the order of nanometres and L of millimetres or centimetres, these lengths are henceforth assumed to satisfy the strong inequality $\epsilon \stackrel{\mathrm{def}}{=} l/L \ll 1$. The essence of the asymptotic approach presented here consists of recognizing that the diffuse, three-dimensional, interfacial transition region seen by the microscale observer will only truly become a two-dimensional macroscale singular surface in the formal mathematical limit $\epsilon \to 0$.

Because of the existence of the two very disparate length scales l and L over which significant continuum field changes occur, interfacial systems are amenable to theoretical analysis by the method of matched asymptotic expansions, with the parameter ϵ playing the role of a small parameter in the perturbation analysis of the exact, microscale transport equations. Only the first-order terms in this perturbation, found by taking the limit as $\epsilon \to 0$, are essential, considering the above premise upon which the present work is based. Such an analysis will provide a systematic and rational method for deriving the pertinent *macroscale*, surface-excess, interfacial conservation and constitutive transport equations (together with the macroscale interfacial phenomenological coefficients appearing in the latter) from a knowledge of the comparable *microscale* conservation and constitutive equations and their volumetric phenomenological material functions. Trivially, one concurrently obtains the 'bulk' conservation and constitutive equations, as well as the corresponding phenomenological functions, that characterize the immiscible fluids lying on either side of the singular surface. Our methods will prove to be valid not only for material interfaces but also for non-material phase interfaces.

In this paper (Part I), an asymptotic method for analysing systems containing moving and deforming interfaces is developed. This method provides a rational, mathematical reconciliation of the micro- and macroscale views of the interface. The fundamental generic conservation equations for the two-dimensional macroscale interface (as well as for the two bulk-fluid regions on either side of the interface) are then derived from the corresponding microscale equations. The derivation of macroscale interfacial constitutive equations is discussed in Part II (the following paper).
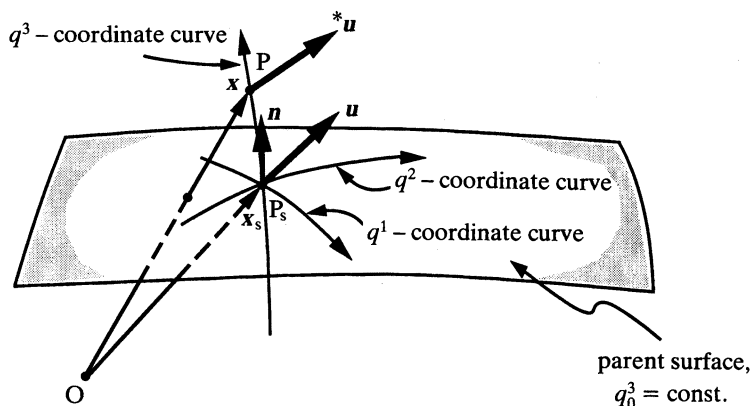
Figure 2. Surface-fixed coordinate system used to parametrize euclidean physical space. A point P_s 'fixed' on the coordinate parent surface is represented by the instantaneous position vector $\boldsymbol{x}_s \equiv \boldsymbol{x}_s(q^1, q^2, t)$ originating from the space-fixed origin O. The velocity of P_s as seen by a space-fixed observer at O is given by the vector $\boldsymbol{u}$, and the unit normal to the surface at P_s by the vector $\boldsymbol{n}$. An arbitrary point P in physical space is represented by the position vector $\boldsymbol{x} \equiv \boldsymbol{x}(\boldsymbol{x}_s, q^3, t)$ originating from the origin O. (Since the q^3-coordinate curves can change with time, the variable t in the argument is not redundant.) In this parametrization, the unit tangent vector to the q^3-coordinate curve is defined to be perpendicular to the parent surface, and thus equivalent to $\boldsymbol{n}$, at every point P_s on the parent surface. The velocity of the surface-fixed coordinate system at P as seen by a space-fixed observer at O is given by $^*\boldsymbol{u}$.

2. Surface-fixed coordinate system

The development of macroscale equations for systems containing mobile interfaces is facilitated by parameterizing the three-dimensional physical space domain containing the interfacial system via use of a surface-fixed coordinate system (see figure 2). Such a system is affixed to a two-dimensional riemannian coordinate reference (or parent) surface, which may move and deform within conventional three-dimensional physical space, the latter here assumed to be euclidean. This parameterization is not based upon defining material points; thus, the possibility of mass transport across the interface is not excluded. Instead, the surface-fixed coordinate system parameterization depends only upon the construction of a non-material, time-dependent coordinate parent surface which coincides with the two-dimensional macroscale interface at all times.

The interfacial system is assumed to be embedded in three-dimensional euclidean physical space. An arbitrary point P in physical space will be uniquely defined (with respect to an inertial reference frame centred at the origin O) by the position vector $\boldsymbol{x}$ originating at O and terminating at P. A point will be considered to be space-fixed if its position vector remains constant throughout all time in this inertial reference frame.

The surface-fixed coordinate system is affixed to a two-dimensional moving and deforming coordinate parent surface. This parent surface is so constructed as to coincide at all times with the two-dimensional physical macroscale interface. From the microscale point of view, such a construction implies that the parent surface must lie somewhere within the interfacial transition region. In the asymptotic theory presented here, the precise location of the parent surface is unimportant so long as it lies within the inner region, wherein steep material property and concomitant field changes occur. (For more detail, see §8.) In addition, the parent surface is required

to be completely defined at the macroscale. Thus, the two principal curvatures κ_1 and κ_2 of the surface must satisfy the scaling relation

$$|\kappa_\alpha| L = O(1) \quad (\alpha = 1, 2) \tag{2.1}$$

at every point on the parent surface, even at the microscale. This condition will limit the applicability of the subsequent theory to situations for which the curvature of the interface is a strictly macroscale quantity, i.e. $\leqslant O(L^{-1})$.

Every point on the parent surface can be arbitrarily parametrized by a pair of curvilinear coordinates (q^1, q^2) intrinsic to the surface. A point on the parent surface will be defined as surface-fixed if its q^1 and q^2 values remain constant.† A surface-fixed point P_s will be represented in physical space by the position vector $\boldsymbol{x}_s$ which originates at the space-fixed origin O and terminates at P_s. This vector can be determined uniquely for all times by the relation

$$\boldsymbol{x}_s = \boldsymbol{x}_s(q^1, q^2, t), \tag{2.2}$$

where the time dependence arises from the dynamic nature of the macroscale interface and/or the coordinate parametrization with respect to the space-fixed origin. The velocity $\boldsymbol{u}$ of the surface-fixed point P_s as seen by a space-fixed observer is defined by the expression

$$\boldsymbol{u} = \left(\frac{\partial \boldsymbol{x}_s}{\partial t}\right)_{q^1, q^2}, \tag{2.3}$$

and will be termed the parent surface coordinate velocity.

Several other pertinent geometric quantities characterizing the parent surface must be defined. In particular, the unit vector normal to the coordinate parent surface will be denoted by $\boldsymbol{n}$ (which will be chosen to point in the direction for which the vector set $(\boldsymbol{a}_1, \boldsymbol{a}_2, \boldsymbol{n})$ is right-handed, with $\boldsymbol{a}_1$ and $\boldsymbol{a}_2$ respective vectors tangent to the q^1- and q^2-coordinate curves and pointing in the direction of increasing q^α values (see Appendix A)), the surface idemfactor by $\boldsymbol{I}_s \equiv \boldsymbol{I} - \boldsymbol{nn}$, and the surface gradient operator by $\nabla_s \equiv \boldsymbol{I}_s \cdot \nabla$ (Brenner 1979). The (symmetric) curvature dyadic for the parent surface is defined by the relation $\boldsymbol{b} = -\nabla_s \boldsymbol{n}$; and the algebraically-signed mean curvature H of the surface (which is positive when the mean curvature is concave in the direction of $\boldsymbol{n}$) has the form $H = -\frac{1}{2}\nabla_s \cdot \boldsymbol{n}$ (Eliassen 1963).

In order to parametrize all of physical space at any instant in time, an additional coordinate variable q^3, say, is needed. The choice of the q^3-coordinate curve (formed by the intersection of the pair of surfaces on which q^1 and q^2 are each respectively constant) is governed by the physical nature of the interfacial system. At the microscale level of description, extremely large changes in the values of the continuum fields characterizing the system may occur in the direction normal to the parent surface. On the other hand, in all but pathological circumstances, only

---

† Since the reference surface may move and deform within conventional three-dimensional physical space, the concept of a surface-fixed point is somewhat arbitrary when viewed from physical space. For example, consider the coordinate parametrization of the surface of a motionless spherical droplet. One could, arbitrarily, define the spherical-coordinate reference surface to be undergoing solid-body rotation about its centre when viewed by a space-fixed observer. Most surface-fixed points will then have a tangential velocity component (even though the material points composing the sphere surface are, in fact, motionless) according to a space-fixed observer. However, the normal velocity component of a surface-fixed point is determined by the restriction that the reference surface must coincide with the macroscale interface. Thus, one way to unambiguously define a surface-fixed point is to constrain its motion to be perpendicular to the surface. In the interest of generality, however, such a constraint will not be imposed upon a surface-fixed point.

relatively small changes in field variables occur in directions tangential to the surface. To emphasize the importance of the normal direction, all q^3-coordinate curves will be constrained to follow a normal trajectory to the coordinate parent surface, with q^3 increasing in the direction of $\boldsymbol{n}$. The parent surface itself will be defined by the equation $q^3 = q_0^3$, where q_0^3 is a constant. Since both a macroscale and a microscale observer must be able to produce an equivalent coordinate parameterization, the q^3-coordinate curves are required to be completely defined at the macroscale in the sense that the curvature $*\kappa$ of all q^3-coordinate curves must satisfy the relation

$$|*\kappa|\, L = O(1) \tag{2.4}$$

at every point along the coordinate curve, even at the microscale. (For a parallel surface parameterization (Eliassen 1963), $*\kappa = 0$, thus satisfying (2.4) trivially.) (An asterisk preceding a symbol will be used throughout this paper to distinguish geometric variables defined at an arbitrary point (q^1, q^2, q^3) in physical space from the corresponding variables defined on the coordinate parent surface $q^3 = q_0^3 = \text{constant}$ for the same value of (q^1, q^2).) Each of the q^3-coordinate surfaces, namely the family of surfaces upon which $q^3 = \text{constant}$ (and hence over which only q^1 and q^2 vary), will be defined to be orthogonal to the q^3-coordinate curves, thus creating a semi-orthogonal coordinate system. Within the interfacial transition region, the two principal curvatures $*\kappa_1$ and $*\kappa_2$ of each q^3-coordinate surface are assumed to satisfy the relation

$$|*\kappa_\alpha|\, L = O(1) \quad (\alpha = 1, 2) \tag{2.5}$$

at every point on the q^3-coordinate surface, even at the microscale.

Using this parameterization, any point in three-dimensional physical space can be represented by the position vector

$$\boldsymbol{x} = \boldsymbol{x}(q^1, q^2, q^3, t) \equiv \boldsymbol{x}(\boldsymbol{x}_\mathrm{s}, q^3, t) \tag{2.6}$$

originating at the space-fixed origin O. The velocity of the surface-fixed coordinate system at a point P as seen by a space-fixed observer is given by the expression

$$*\boldsymbol{u} = \left(\frac{\partial \boldsymbol{x}}{\partial t}\right)_{q^1, q^2, q^3} \tag{2.7}$$

and will be termed the coordinate velocity. We shall require that the coordinate velocity $*\boldsymbol{u}$ be a macroscale quantity that changes only relatively slowly over microscale distances; explicitly,

$$\left(\frac{L}{U}\right)\nabla *\boldsymbol{u} = O(1), \tag{2.8}$$

where the scalar U is a characteristic velocity of the interfacial system.

As with the coordinate parent surface, some important geometric quantities serving to characterize an arbitrary q^3-coordinate surface must be defined, such quantities being distinguished by an asterisk from the analogous quantities existing on the parent surface. Thus, the unit vector normal to a q^3-coordinate surface will be denoted by $*\boldsymbol{n}$, the q^3-coordinate surface idemfactor by $*\boldsymbol{I}_\mathrm{s} = \boldsymbol{I} - *\boldsymbol{n}*\boldsymbol{n}$, and the q^3-coordinate surface gradient operator by $*\nabla_\mathrm{s} = *\boldsymbol{I}_\mathrm{s} \cdot \nabla$. The curvature dyadic $*\boldsymbol{b}$ for a q^3-coordinate surface, defined by the relation

$$*\boldsymbol{b} = - *\nabla_\mathrm{s}*\boldsymbol{n}, \tag{2.9}$$

is symmetric. As such, it can be written in the canonical, 'diagonalized' form

$$*\boldsymbol{b} = *\kappa_1 \, *\boldsymbol{e}_{(1)} \, *\boldsymbol{e}_{(1)} + *\kappa_2 \, *\boldsymbol{e}_{(2)} \, *\boldsymbol{e}_{(2)}, \tag{2.10}$$

where $*\kappa_1$ and $*\kappa_2$ are the (algebraically-signed) principal curvatures of the q^3-coordinate surface (i.e. the eigenvalues of the curvature dyadic), and the unit vectors $*\boldsymbol{e}_{(1)}$ and $*\boldsymbol{e}_{(2)}$ are the principal directions of curvature of the q^3-coordinate surface (i.e. the normalized eigenvectors of $*\boldsymbol{b}$). In terms of the principal curvatures, the algebraically-signed mean curvature $*H$ of the q^3-coordinate surface adopts the classical form

$$*H \overset{\text{def}}{=} \tfrac{1}{2} *\boldsymbol{I}_{\text{s}} : *\boldsymbol{b} \equiv -\tfrac{1}{2} *\nabla_{\text{s}} \cdot *\boldsymbol{n} = \tfrac{1}{2}(*\kappa_1 + *\kappa_2). \tag{2.11}$$

The distance or arc length n along the q^3-coordinate curve, as measured from the parent surface (with $n = 0$ at the parent surface $q^3 = q_0^3$) in the direction of increasing q^3, plays an important role in the subsequent perturbation analysis. A differential element of arc length $\mathrm{d}n$ along the q^3-coordinate curve is related to the differential displacement $\mathrm{d}q^3$ by the expression (cf. (A 22))

$$\mathrm{d}n = *h_3 \, \mathrm{d}q^3 \quad (*h_3 > 0), \tag{2.12}$$

where $*h_3(\boldsymbol{x}_{\text{s}}, q^3, t)$ is the metrical coefficient (Happel & Brenner 1986, p. 476) for the q^3-coordinate curve. Accordingly, the distance n can be determined by the integral relation

$$n = \int_{q_0^3}^{q^3} *h_3 \, \mathrm{d}q^3. \tag{2.13}$$

(To avoid circumlocution, we have deleted the prime that would normally have appeared in the dummy variable $q^{3'}$ occurring in the integrand of (2.13). This scheme will be consistently followed throughout the subsequent text.) Because of the role played in the subsequent theory by the intrinsic variable n, the coordinate variable set $(\boldsymbol{x}_{\text{s}}, q^3)$ appearing in the arguments of the various field variables will often be replaced by the alternate variable set $(\boldsymbol{x}_{\text{s}}, n)$. However, when replacing q^3 by n, it must be borne in mind that surfaces of constant n are not necessarily equivalent to surfaces of constant q^3. (Surfaces of constant n are only equivalent to q^3-coordinate surfaces in circumstances for which $*h_3$ is independent of q^1, q^2, and t. Such conditions hold for the special case of parallel surfaces (Eliassen 1963), for which $*h_3 = 1$. This fact partially accounts for the special significance of the parallel-surface parametrization.)

Since the q^3-coordinate curve is defined such as to follow an orthogonal trajectory to the q^3-coordinate surfaces, the unit tangent vector to the q^3-coordinate curve is equivalent to $*\boldsymbol{n}$, the unit normal to the q^3-coordinate surface. Thus, the curvature $*\kappa$, as well as the principal unit normal vector $*\boldsymbol{p}$ of a q^3-coordinate curve, may be derived from the properties of $*\boldsymbol{n}$ via the relation (McConnell 1957, p. 159)

$$*\boldsymbol{n} \cdot (\nabla *\boldsymbol{n}) \equiv \partial *\boldsymbol{n}/\partial n = *\kappa \, *\boldsymbol{p}. \tag{2.14}$$

A surface-fixed coordinate parametrization of physical space by the variables (q^1, q^2, q^3) will be unique at each point so long as the jacobian

$$J = \left(\frac{\partial \boldsymbol{x}}{\partial q^1}\right) \cdot \left[\left(\frac{\partial \boldsymbol{x}}{\partial q^2}\right) \times \left(\frac{\partial \boldsymbol{x}}{\partial q^3}\right)\right] \tag{2.15}$$
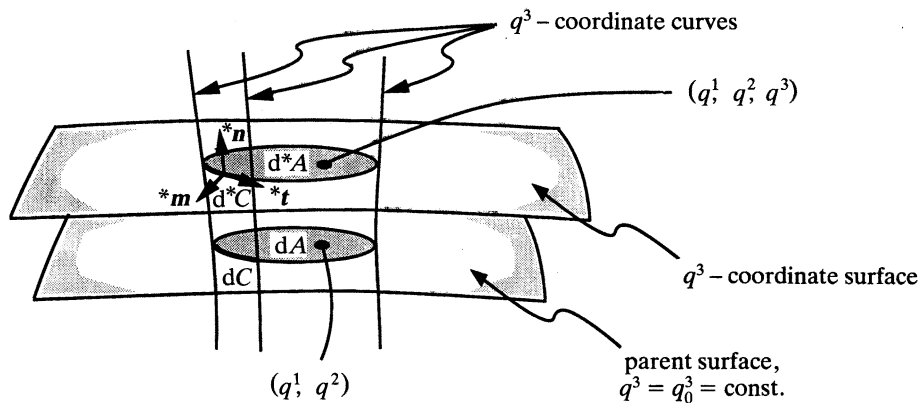
Figure 3. 'Projection' of the differential elements d*A and d*C onto the coordinate parent surface along an 'envelope' determined by the q^3-coordinate curves. Also shown are the unit normal vector *n to the q^3-coordinate surface, the unit tangent vector *t to the curve d*C, and the unit surface vector *m = *t × *n, lying normal to the curve d*C in the tangent plant of the q^3-coordinate surface.

is non-vanishing at that point. The existence of the jacobian is assured (except possibly at isolated points outside the interfacial region) by virtue of the fact that each point in space is parametrized by some triplet of values (q^1, q^2, q^3). A unique parameterization of physical space is strictly necessary only in the neighbourhood of the interfacial transition region. As such, J can, in fact, vanish at points far from the interfacial transition region without negating the subsequent theory. For situations in which (2.1) holds, such a parameterization can always be constructed using parallel surfaces (Eliassen 1963).

A differential areal element d*A centred at a point (q^1, q^2, q^3) lying upon an arbitrary q^3-coordinate surface can be written as (cf. (B 2) and (B 22))

$$\mathrm{d}*A = *M(x_s, q^3)\,\mathrm{d}A \tag{2.16}$$

in terms of the corresponding differential areal element d*A* centred at the point (q^1, q^2) on the parent surface (figure 3). Here, d*A* is determined by projecting the element d*A onto the parent surface along an envelope determined by the q^3-coordinate curves; moreover, $M*(x_s, q^3)$ is the areal magnification factor given by

$$*M = \exp\left(-\int_{q_0^3}^{q^3} 2*H*h_3\,\mathrm{d}q^3\right). \tag{2.17}$$

The analogous relationship governing the projection onto the parent surface of a differential element of length d*C lying upon an arbitrary q^3-coordinate surface is given by the expression (cf. (B 24), (B 32) and (B 33))

$$\mathrm{d}*C = *N(x_s, q^3)\,\mathrm{d}C. \tag{2.18}$$

Here, d*C is the differential lineal element on the parent surface, found by projecting the element d*C onto the parent surface along lines corresponding to the q^3-coordinate curves (figure 3). In the above, $N*(x_s, q^3)$ is the lineal magnification factor given by

$$*N = \exp\left(-\int_{q_0^3}^{q^3} *\kappa_{(n)}(*t)\,*h_3\,\mathrm{d}q^3\right), \tag{2.19}$$

with the scalar

$$*\kappa_{(n)}(*t) = *t*t : \boldsymbol{b} \tag{2.20}$$

the normal curvature (McConnell 1957, p. 210) of the q^3-coordinate surface in the direction of $*t$, the latter being the unit tangent vector to the curve d$*C$. (For multiple vector operations, the nesting convention (Chapman & Cowling 1961) is used. According to this convention, the operations are performed, *inter alia*, from the inside outward, such that $\boldsymbol{ab} : \boldsymbol{cd} = (\boldsymbol{b} \cdot \boldsymbol{c})(\boldsymbol{a} \cdot \boldsymbol{d})$, where $\boldsymbol{a}, \boldsymbol{b}, \boldsymbol{c}$, and $\boldsymbol{d}$ are vectors.) Also related to this curve is the unit vector $*\boldsymbol{m} = *t \times *\boldsymbol{n}$, which is normal to d$*C$ and lies in the tangent plane of the q^3-coordinate surface. This vector can be written as (cf. (B 42))

$$*\boldsymbol{m} = \boldsymbol{m} - \int_{q_0^3}^{q^3} (*t*t + *\boldsymbol{n}*\boldsymbol{n}) \cdot (\nabla *\boldsymbol{n}) \cdot *\boldsymbol{m} *h_3 \, \mathrm{d}q^3. \tag{2.21}$$

Since the (macroscale) interface moves and deforms with time, the instantaneous parametrization $\boldsymbol{x} \equiv \boldsymbol{x}(\boldsymbol{x}_{\mathrm{s}}, n, t)$ of physical space by the surface-fixed coordinate system must be performed for each successive instant in time. This time-dependent parametrization must be effected such that all pertinent geometric functions are continuous throughout time. In order to simplify subsequent notion, derivatives with respect to time holding the surface-fixed coordinates (q^1, q^2, q^3) constant will be represented by the operator

$$\frac{\delta}{\delta t} \overset{\mathrm{def}}{=} \left(\frac{\partial}{\partial t}\right)_{q^1, q^2, q^3}, \tag{2.22}$$

which will be termed the coordinate-convected time derivative. This derivative can be written as

$$\frac{\delta}{\delta t} = \left(\frac{\partial}{\partial t}\right)_{\boldsymbol{x}} + *\boldsymbol{u} \cdot \nabla, \tag{2.23}$$

in terms of the space-fixed time derivative $(\partial/\partial t)_{\boldsymbol{x}}$. On the parent surface $q^3 = q_0^3$, the coordinate-convected time derivative will be notationally represented by the symbol

$$\frac{\delta_{\mathrm{s}}}{\delta t} \overset{\mathrm{def}}{=} \left(\frac{\partial}{\partial t}\right)_{q^1, q^2, q_0^3}, \tag{2.24}$$

which will be termed the coordinate-convected surface time derivative.

3. Singular perturbation analysis

Consider a generic, continuum, tensorial, microscale field $\boldsymbol{\lambda} \equiv \boldsymbol{\lambda}(\boldsymbol{x})$ (e.g. a volumetric density of some extensive physical property) defined at every point $\boldsymbol{x}$ of the system. (For simplicity and focus, the functional time dependence of $\boldsymbol{\lambda}$, if any, has been explicitly suppressed in its argument.) This field, which can equivalently be represented as $\boldsymbol{\lambda} = \boldsymbol{\lambda}(\boldsymbol{x}_{\mathrm{s}}, n)$ in terms of the surface-fixed coordinate system, is assumed to be a continuous function of position – in particular of the distance n – throughout the entire domain occupied by the fluid. Within the two bulk-fluid regions, and for a fixed value of $\boldsymbol{x}_{\mathrm{s}}$, the field $\boldsymbol{\lambda}$ will generally change only gradually with n; however, within the interfacial transition region, $\boldsymbol{\lambda}$ may undergo rapid changes with n. (For example, if $\boldsymbol{\lambda}$ represents the microscale mass density ρ in an

immiscible oil–water system possessing significantly different bulk densities, ρ will then be sensibly constant throughout each separate bulk phase. However, in immediate proximity to the interface, ρ will change quite rapidly in magnitude with n, from the bulk-phase density of oil to that of water.)

Upon using the respective characteristic lengths l and L of the interfacial and bulk-fluid regions, the non-dimensional normal distance

$$\tilde{n} \stackrel{\text{def}}{=} n/l, \tag{3.1}$$

which is characteristic of microscale distances, and

$$\bar{n} \stackrel{\text{def}}{=} n/L \equiv \epsilon \tilde{n}, \tag{3.2}$$

which is characteristic of macroscale distances, can respectively be defined. In the latter equation the characteristic length ratio

$$\epsilon \stackrel{\text{def}}{=} l/L \ll 1 \tag{3.3}$$

is assumed to satisfy the indicated inequality, and hence serve as a small (non-negative) parameter in the subsequent perturbation analysis.

Within the interfacial region, the microscale field λ may change significantly over distances of $O(l)$, i.e. with $O(1)$ changes in $\tilde{n}$. Explicitly, $\partial\lambda/\partial\tilde{n}$ may be of $O(1)$ for $|\tilde{n}| = O(1)$. The functional form

$$\lambda = \lambda(x_{\rm s}, \tilde{n}; \epsilon) \tag{3.4}$$

is thus a useful representation for those spatial positions x lying within the interfacial transition region. In this form, changes, $\Delta\lambda$, in the value of λ occurring over the microscale distance $|\Delta\tilde{n}| = O(1)$ can be distinguished. Gradual changes in λ, if any, occurring within the bulk-field regions will occur only over distances $|\Delta\tilde{n}| \equiv O(\epsilon^{-1})$. (Here and hereafter, the equivalence symbol appearing in the expression $\equiv O(\ )$ is used to indicate 'exactly equal to the specific order'. In other words, the statement $f(\epsilon) \equiv O[g(\epsilon)]$ as $\epsilon \to 0$ is true if there exist two positive numbers A and B, independent of ϵ, and an $\epsilon_0 > 0$ such that $A|g(\epsilon)| \leqslant |f(\epsilon)| \leqslant B|g(\epsilon)|$ for all $|\epsilon| \leqslant \epsilon_0$. However, for the statement $f(\epsilon) = O[g(\epsilon)]$ as $\epsilon \to 0$ to be true, the only constraint imposed upon $f(\epsilon)$ is that $|f(\epsilon)| \leqslant B|g(\epsilon)|$ for all $|\epsilon| \leqslant \epsilon_o$.)

Sensible changes, if any, in the respective values of λ within the two bulk-fluid regions, $|\bar{n}| = O(1)$ lying on either side of the interfacial region, will occur only over the much larger length scale $|\Delta\bar{n}| \equiv O(1)$. The functional form

$$\lambda = \lambda(x_{\rm s}, \bar{n}; \epsilon) \tag{3.5}$$

is thus more useful than (3.4) for those positions x lying within these bulk-fluid regions. In this form, changes, $\Delta\lambda$, in λ occurring over macroscale distances – corresponding to $|\Delta\bar{n}| \equiv O(1)$ – can be distinguished. In general, any rapid changes in λ within the interfacial transition region will occur over distances characterized by $|\Delta\bar{n}| = O(\epsilon)$. As $\epsilon \to 0$, such changes will appear to occur discontinuously when the functional form (3.5) is used in a regular perturbation expansion scheme that utilizes ϵ as the small perturbation parameter.

Expansion of the field λ with respect to the small parameter ϵ is the first step towards application of singular perturbation techniques to the interfacial system.

Separate expansions must be performed within the interfacial transition region and within the two bulk-fluid regions lying on either side of the latter. In the terminology of singular perturbation theory (Nayfeh 1973), the interfacial region – defined by $|\tilde{n}| = O(1)$ – constitutes the inner region, whereas the two bulk-fluid regions – defined by $|\bar{n}| \equiv O(1)$ – constitute the outer regions.

The inner perturbation expansion of λ in terms of the small parameter ϵ, valid within the interfacial transition region, is performed on the basis of the functional form (3.4), keeping $\tilde{n}$ (and $\boldsymbol{x}_s$) fixed:

$$\lambda(\boldsymbol{x}_s, \tilde{n}; \epsilon) = \tilde{\lambda}(\boldsymbol{x}_s, \tilde{n}) + \tilde{\lambda}_R(\boldsymbol{x}_s, \tilde{n}; \epsilon), \tag{3.6}$$

where

$$\tilde{\lambda}(\boldsymbol{x}_s, \tilde{n}) \overset{\text{def}}{=} \lim_{\substack{\epsilon \to 0 \\ \tilde{n}\,\text{fixed}}} \lambda(\boldsymbol{x}_s, \tilde{n}; \epsilon) \tag{3.7}$$

represents the leading-order term in this expansion. (For simplicity we depart here from standard notation (Kevorkian & Cole 1981), which would require that what here is called $\tilde{\lambda}$ be called $\tilde{\lambda}_0$; that is, ordinarily one deals with the complete inner expansion to all orders in ϵ, namely

$$\tilde{\lambda}(\boldsymbol{x}_s, \tilde{n}; \epsilon) \overset{\text{def}}{=} \lambda(\boldsymbol{x}_s, \bar{n} = \tilde{n}\epsilon; \epsilon),$$

whence

$$\tilde{\lambda}(\boldsymbol{x}_s, \tilde{n}; \epsilon) = \tilde{\lambda}_0(\boldsymbol{x}_s, \tilde{n}) + \tilde{f}_1(\epsilon)\,\tilde{\lambda}_1(\boldsymbol{x}_s, \tilde{n}) + \tilde{f}_2(\epsilon)\,\tilde{\lambda}_2(\boldsymbol{x}_s, \tilde{n}) + \dots,$$

where $\tilde{f}_k(\epsilon) \to 0$ and $\tilde{f}_{k+1}/\tilde{f}_k \to 0$ as $\epsilon \to 0$, and $\tilde{\lambda}_{k-1} = O(1)$ $(k = 1, 2, 3, \dots)$. Since, however, these higher-order terms will not be addressed here, we can confound $\tilde{\lambda}(\boldsymbol{x}_s, \tilde{n}; \epsilon)$ with its leading-order term, namely $\tilde{\lambda}_0(\boldsymbol{x}_s, \tilde{n})$ (and simply refer to the latter as $\tilde{\lambda}(\boldsymbol{x}_s, \tilde{n})$). The remaining, higher-order terms are assigned to the remainder function, $\tilde{\lambda}_R(\boldsymbol{x}_s, \tilde{n}; \epsilon)$.) All remaining higher-order terms in (3.6) are contained in the 'remainder' function $\tilde{\lambda}_R$, which necessarily satisfies the constraint

$$\lim_{\substack{\epsilon \to 0 \\ \tilde{n}\,\text{fixed}}} \tilde{\lambda}_R(\boldsymbol{x}_s, \tilde{n}; \epsilon) = \boldsymbol{0}. \tag{3.8}$$

The term $\tilde{\lambda}$ can be used to asymptotically approximate λ within the inner region; explicitly,

$$\lambda = \tilde{\lambda}[1 + o(1)] \quad \text{for } |n| = O(1). \tag{3.9}$$

Perturbation expansions of λ in the small parameter ϵ, respectively valid within each of the two outer regions, are performed on the basis of the functional form (3.5), keeping $\bar{n}$ (and $\boldsymbol{x}_s$) fixed

$$\lambda(\boldsymbol{x}_s, \bar{n}; \epsilon) = \bar{\lambda}_1(\boldsymbol{x}_s, \bar{n}) + \bar{\lambda}_{1R}(\boldsymbol{x}_s, \bar{n}; \epsilon) \quad (\bar{n} > 0), \tag{3.10a}$$

$$\lambda(\boldsymbol{x}_s, \bar{n}; \epsilon) = \bar{\lambda}_2(\boldsymbol{x}_s, \bar{n}) + \bar{\lambda}_{2R}(\boldsymbol{x}_s, \bar{n}; \epsilon) \quad (\bar{n} < 0), \tag{3.10b}$$

wherein

$$\bar{\lambda}_1(\boldsymbol{x}_s, \bar{n}) \overset{\text{def}}{=} \lim_{\substack{\epsilon \to 0 \\ \bar{n}\,\text{fixed}}} \lambda(\boldsymbol{x}_s, \bar{n}; \epsilon) \quad (\bar{n} > 0) \tag{3.11a}$$

and

$$\bar{\lambda}_2(\boldsymbol{x}_s, \bar{n}) \overset{\text{def}}{=} \lim_{\substack{\epsilon \to 0 \\ \bar{n}\,\text{fixed}}} \lambda(\boldsymbol{x}_s, \bar{n}; \epsilon) \quad (\bar{n} < 0) \tag{3.11b}$$

constitute the leading-order terms in each of the respective expansions. All remaining higher-order terms are embodied within the 'remainder' functions $\bar{\lambda}_{1R}$ and $\bar{\lambda}_{2R}$, which are assumed to possess the property that

$$\lim_{\substack{\epsilon \to 0 \\ \bar{n} \text{ fixed}}} \bar{\lambda}_{\alpha R}(\boldsymbol{x}_s, \bar{n}; \epsilon) = \boldsymbol{0} \quad (\alpha = 1, 2). \tag{3.12}$$

The respective leading-order outer fields $\bar{\lambda}_1$ and $\bar{\lambda}_2$ can be used to approximate $\boldsymbol{\lambda}$ within the appropriate outer regions; explicitly,

$$\boldsymbol{\lambda} = \bar{\lambda}_1[1 + o(1)] \quad \text{for } |\bar{n}| \gg O(\epsilon) \quad (\bar{n} > 0), \tag{3.13a}$$

$$\boldsymbol{\lambda} = \bar{\lambda}_2[1 + o(1)] \quad \text{for } |\bar{n}| \gg O(\epsilon) \quad (\bar{n} < 0). \tag{3.13b}$$

In general, the outer field $\bar{\lambda}$ may be discontinuous across the interface; that is,

$$[\![\bar{\lambda}]\!] \stackrel{\text{def}}{=} \lim_{\bar{n} \to 0+} \bar{\lambda}_1(\boldsymbol{x}_s, \bar{n}) - \lim_{\bar{n} \to 0-} \bar{\lambda}_2(\boldsymbol{x}_s, \bar{n}) \neq \boldsymbol{0} \tag{3.14}$$

in general, with the double brackets $[\![\ldots]\!]$ denoting the algebraically-signed 'interfacial jump' occurring in the value of the outer field appearing within the enclosed argument.

Throughout this paper, a tilde will consistently be used to denote inner variables (both dependent and independent), and an overbar to denote outer variables. In addition, only the lowest-order terms in ϵ will be retained.

Products of the dependent variables will appear in the subsequent microscale theory. Since the limit of the product of two functions is equal to the product of the limits (cf. Thomas & Finney 1980) so long as all limits exist, we can write

$$\overline{\boldsymbol{a}\boldsymbol{b}} = \bar{\boldsymbol{a}}\bar{\boldsymbol{b}}, \tag{3.15}$$

for the outer limit, where $\boldsymbol{a}(\boldsymbol{x}_s, \bar{n}; \epsilon)$ and $\boldsymbol{b}(\boldsymbol{x}_s, \bar{n}; \epsilon)$ are arbitrary functions possessing definable outer limits $\bar{\boldsymbol{a}}$ and $\bar{\boldsymbol{b}}$. Similarly, for the inner limit,

$$\widetilde{\boldsymbol{a}\boldsymbol{b}} = \tilde{\boldsymbol{a}}\tilde{\boldsymbol{b}}, \tag{3.16}$$

where $\boldsymbol{a}(\boldsymbol{x}_s, \tilde{n}, \epsilon)$ and $\boldsymbol{b}(\boldsymbol{x}_s, \tilde{n}; \epsilon)$ are arbitrary functions possessing definable inner limits $\tilde{\boldsymbol{a}}$ and $\tilde{\boldsymbol{b}}$.

Lying between the inner, interfacial transition region and the two outer, bulk-fluid regions are two intermediate overlap regions, within which both the outer and inner expansions are each assumed to be equally valid in an asymptotic sense. The dimensionless normal distance,

$$\hat{n} \stackrel{\text{def}}{=} \epsilon^{-r}\bar{n} = \epsilon^{1-r}\tilde{n} \quad (0 < r < 1) \tag{3.17}$$

with r some constant, is defined to be of $O(1)$ within these intermediate regions. The two limiting values bounding r correspond to $\hat{n}$ being identical with $\tilde{n}$ (when $r = 1$) and $\bar{n}$ (when $r = 0$). These limits on r may become tighter in specific applications, depending upon the exact functional form of the field $\boldsymbol{\lambda}$. Since both the outer and inner expansions are assumed mutually valid within the two intermediate regions, $|\hat{n}| \equiv O(1)$, the pair of matching conditions

$$\lim_{\substack{\epsilon \to 0 \\ \hat{n} \text{ fixed}}} \bar{\lambda}_1(\boldsymbol{x}_s, \bar{n} = \epsilon^r \hat{n}) = \lim_{\substack{\epsilon \to 0 \\ \hat{n} \text{ fixed}}} \tilde{\lambda}(\boldsymbol{x}_s, \tilde{n} = \epsilon^{r-1}\hat{n}) \quad (\hat{n} > 0) \tag{3.18a}$$

and $$\lim_{\substack{\epsilon \to 0 \\ \hat{n} \, \text{fixed}}} \bar{\lambda}_2(x_s, \bar{n} = \epsilon^r \hat{n}) = \lim_{\substack{\epsilon \to 0 \\ \hat{n} \, \text{fixed}}} \tilde{\lambda}(x_s, \tilde{n} = \epsilon^{r-1}\hat{n}) \quad (\hat{n} < 0) \qquad (3.18b)$$

for the inner and outer expansions must hold for all x_s. Clearly, as $\epsilon \to 0$ with $\hat{n}$ fixed, $\bar{n} \equiv O(\epsilon^r) \to \pm 0$ whereas $\tilde{n} \equiv O(\epsilon^{r-1}) \to \pm \infty$.

(a) Order-of-magnitude scaling relations for important geometric properties

Table 1 provides a tabulation of order-of-magnitude values within each of the three distinct microscale domains for the three dimensionless normal distances, as derived from the three respective definitions (3.1), (3.2), and (3.17).

Order-of-magnitude values existing within the inner and intermediate regions can now be determined for the relevant geometric parameters appearing in §2. Upon utilizing (2.4), (2.5), (2.10), (2.11), and (2.14), the scaling relations

$$*bL = O(1), \qquad (3.19)$$

$$*HL = O(1), \qquad (3.20)$$

$$*n \cdot (\nabla *n) L = O(1) \qquad (3.21)$$

are found to apply within both the inner and intermediate regions. Substitution of (2.12) into (2.17) yields

$$*M = \exp\left[-\epsilon \int_0^{\tilde{n}} 2(*HL) \, d\tilde{n}\right]. \qquad (3.22)$$

Similarly, (2.19) adopts the form

$$*N = \exp\left[-\epsilon \int_0^{\tilde{n}} L*\kappa_{(n)}(*t) \, d\tilde{n}\right], \qquad (3.23)$$

where, from (2.20) and (3.19),

$$L*\kappa_{(n)}(*t) = *t*t : (*bL) = O(1) \qquad (3.24)$$

within both the inner and intermediate regions. Perform a Taylor series expansion of (3.22) and (3.23) and subsequently use the order-of-magnitude expressions (3.20) and (3.24), together with the scalings cited in table 1, thereby obtaining the order estimates

$$*M = 1 + O(\epsilon), \quad *N = 1 + O(\epsilon), \qquad (3.25a, b)$$

valid within the inner region, and

$$*M = 1 + O(\epsilon^r), \quad *N = 1 + O(\epsilon^r), \qquad (3.26a, b)$$

valid within the two intermediate regions.

Similar estimates can be derived for $*m$. In this context, substitute (2.12) and (2.9) into (2.21) to obtain

$$*m = m - \epsilon \int_0^{\tilde{n}} (*t*t + *n*n) \cdot (-b + *n*n \cdot \nabla *n) \cdot *mL \, d\tilde{n}. \qquad (3.27)$$

Expand (3.27) via a Taylor series and employ the order-of-magnitude expressions (3.19) and (3.21), together with the appropriate values cited in table 1. This scheme furnishes the estimate

$$*m = m + O(\epsilon), \qquad (3.28)$$

Table 1. *Order-of-magnitude values for the scaled normal distances* $(0 < r < 1)$

scaled normal distance	outer regions	intermediate regions	inner region
outer variable, $\bar{n}$	$O(1)$	$O(\epsilon^r)$	$O(\epsilon)$
intermediate variable, $\hat{n}$	$O(\epsilon^{-r})$	$O(1)$	$O(\epsilon^{1-r})$
inner variable, $\tilde{n}$	$O(\epsilon^{-1})$	$O(\epsilon^{r-1})$	$O(1)$

Table 2. *Identification of generic variables $*f$ and f for specific circumstances*

$*f(x_s, n)$	$f(x_s)$	$\partial *f/\partial \bar{n}$	$\partial *f/\partial \bar{n}$ is $O(1)$ by...
$*n$	n	$(*\kappa L)\,*p$	(2.4)
x/L	x_s/L	$*n$	unit vector
$*u/U$	u/U	$U^{-1}(\partial *u/\partial \bar{n})$	(2.8)

valid within the inner region, and

$$*m = m + O(\epsilon^r), \tag{3.29}$$

valid within the two intermediate regions.

One further expression relating the inner and outer limits of a generic macroscale quantity can be established as follows. Let $*f(x_s, n)$ represent a dimensionless quantity that is defined to be macroscale in the sense that

$$\partial *f/\partial \bar{n} = O(1) \tag{3.30}$$

everywhere, including the interfacial transition region. This function can be written in the integral form

$$*f(x_s, n) = f(x_s) + \int_0^{\bar{n}} \frac{\partial *f}{\partial \bar{n}'}(x_s, \bar{n}'; \epsilon)\, \mathrm{d}\bar{n}', \tag{3.31}$$

wherein

$$f(x_s) \overset{\text{def}}{=} *f(x_s, 0) \tag{3.32}$$

is the value of $*f$ on the parent surface, $n = 0$. Integration of (3.31) using the order-of-magnitude relation (3.30) yields

$$*f(x_s, n) = f(x_s) + \bar{n}O(1) = f(x_s) + \tilde{n}O(\epsilon). \tag{3.33}$$

Form the inner and outer limits, (3.7) and (3.11) respectively, of the above equation to obtain the desired limiting expressions:

$$*\tilde{f}(x_s, \tilde{n}) = f(x_s) = \lim_{\bar{n}\to 0+} *\bar{f}_1(x_s, \bar{n}) = \lim_{\bar{n}\to 0-} *\bar{f}_2(x_s, \bar{n}). \tag{3.34}$$

This relation will prove important in the subsequent analysis of surface-excess phenomena. Table 2 explicitly identifies $*f$ as well as the other relevant variables appearing in the above equations for three important geometric and kinematic parameters.

4. Surface-excess properties

Imagine a macroscale experimentalist who sets about the task of investigating the behaviour of a field variable λ across a fluid interface (which field we will take to be generic). Owing to the relatively coarse scale of resolution of the macroscale
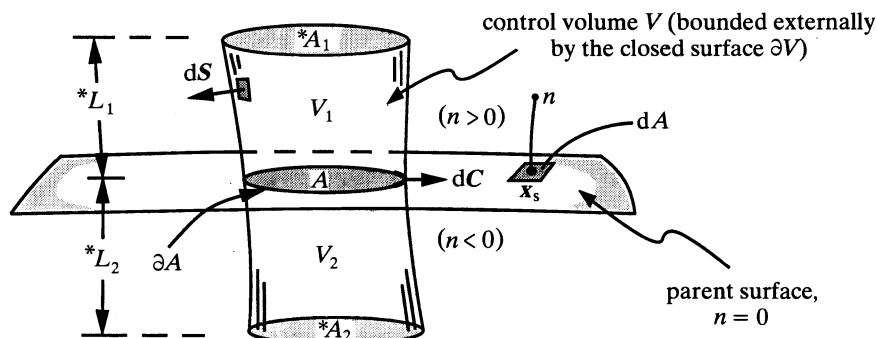
Figure 4. Control volume used to define surface-excess properties. The parent surface ($n = 0$) lies within the interfacial transition region. The control volume $V \equiv V_1 \oplus V_2 \oplus A$ straddles this region and extends well into the two, 'fully developed' bulk-fluid regions. A q^3-coordinate curve envelope laterally bounds the control volume, Lying within the bulk-fluid regions are the upper ($*A_1$) and lower ($*A_2$) end caps, formed by the intersection of q^3-coordinate surfaces with the lateral q^3-coordinate curve envelope. The volumes V_1 and V_2 respectively represent the upper ($n \geqslant 0$) and lower ($n \leqslant 0$) portions of the control volume.

experimental probe, the experimentalist is able to directly measure only the outer, bulk-fluid fields (see figure 1a). This macroscale perspective (in contrast to the microscale perspective depicted in figure 1b) leads her to conclude physically that λ is given at each point x ($\bar{n} \neq 0$) by its bulk-fluid value(s) $\bar{\lambda}$, namely,

$$\lambda \Rightarrow \bar{\lambda} \stackrel{\text{def}}{=} \begin{cases} \bar{\lambda}_1 & (\bar{n} > 0), \\ \bar{\lambda}_2 & (\bar{n} < 0). \end{cases} \tag{4.1}$$

Such a macroscale observer will inevitably believe that each of these separate bulk values $\bar{\lambda}$ is valid right up to the two-dimensional parent surface, $\bar{n} = 0$, though in actuality we recognize these values to be strictly valid only for $|\bar{n}| \gg O(\epsilon)$. Rapid changes, if any, occurring within the diffuse interfacial transition region themselves cannot be explicitly observed by the macroscale observer; they will, however, be implicitly relevant in determining the (macroscale) interfacial jump boundary conditions to be imposed at $\bar{n} = 0$.

Differences existing between the macroscale and microscale views of the transport phenomena can be formally reconciled by assigning *macroscale* surface-excess areal densities λ^s and lineal flux densities $\boldsymbol{\varphi}^s$ of extensive physical properties to each point x_s of the two-dimensional parent surface (and at each instant of time in unsteady-state circumstances). In this section, appropriate expressions for such two-dimensional surface-excess densities will be developed in terms of the corresponding three-dimensional volumetric and areal flux microscale density fields. The symbol $\boldsymbol{\varphi}$ is used in the following discussion to denote generic flux fields so as to avoid any confusion with generic volumetric fields, hereafter represented by the symbol λ. However, all of the relations discussed thus far for the generic field λ apply equally well to $\boldsymbol{\varphi}$.

To develop expressions for the two-dimensional surface-excess densities, consider a moving and deforming surface-fixed control volume $V(t)$, defined as follows (figure 4). Choose an arbitrary areal element A lying on the coordinate parent surface $n = 0$; the closed curve bounding A will be termed ∂A. The q^3-coordinate curves passing through ∂A (cf. figure 3) form the 'sides' of the control volume. Bounding the control

volume at its top and bottom are upper and lower end 'caps', designated respectively by $*A_1$ and $*A_2$, which are conveniently chosen to be q^3-coordinate surfaces that lie well within their respective bulk-fluid regions. Thus, the closed surface ∂V which externally bounds V consists of $*A_1$, $*A_2$, and the q^3-coordinate curve envelope constituting the sides of the volume. The volumes V_1 and V_2 represent the two regions of the control volume lying respectively above ($n > 0$) and below ($n < 0$) the parent surface $n = 0$. Associated with these two volumes are the closed surfaces ∂V_1 and ∂V_2 which respectively bound V_1 and V_2 externally. The closed surface ∂V_1 consists of the two end caps $*A_1$ and A, together with sides determined by the q^3-coordinate curve envelope lying above the parent surface $n = 0$. Similarly, the closed surface ∂V_2 consists of the two end caps $*A_2$ and A, together with sides determined by the q^3-coordinate curve envelope lying below $n = 0$.

Let the continuous variable λ designate the microscale volumetric density field of some extensive property $\mathscr{P}$. The total amount, $\varLambda$, of $\mathscr{P}$ contained within the control volume V at any given time t is given by the expression

$$\varLambda \overset{\text{def}}{=} \int_V \lambda \, \mathrm{d}V. \tag{4.2}$$

A macroscale experimentalist whose instruments traverse the volume V will, however, resolve and hence observe only the macroscale field $\bar{\lambda}$ (cf. (4.1)), thereby concluding that the total amount, $\bar{\varLambda}$, of $\mathscr{P}$ contained within the control volume (at time t) is given rather by

$$\bar{\varLambda} = \int_{V_1} \bar{\lambda}_1 \, \mathrm{d}V + \int_{V_2} \bar{\lambda}_2 \, \mathrm{d}V \equiv \int_V \bar{\lambda} \, \mathrm{d}V. \tag{4.3}$$

Such a macroscale observer will assign to the surface A any disparity that exists between the two amounts $\varLambda$ and $\bar{\varLambda}$, thus obtaining

$$\varLambda^{\mathrm{s}} \overset{\text{def}}{=} \lim_{\epsilon \to 0} (\varLambda - \bar{\varLambda}) \equiv \lim_{\epsilon \to 0} \int_V [\lambda(\boldsymbol{x}_{\mathrm{s}}, n) - \bar{\lambda}(\boldsymbol{x}_{\mathrm{s}}, \bar{n})] \, \mathrm{d}V \tag{4.4}$$

for the surface-excess amount, $\varLambda^{\mathrm{s}}$, of $\mathscr{P}$ assigned to the area A (at time t). Note that we are here formally identifying the mathematical parent surface A with the physical macroscale interface in the $\epsilon \to 0$ limit. A continuous, surface-excess areal density field λ^{s} can now be defined at each point $\boldsymbol{x}_{\mathrm{s}}$ on the interface by the relation

$$\varLambda^{\mathrm{s}} \overset{\text{def}}{=} \int_A \lambda^{\mathrm{s}}(\boldsymbol{x}_{\mathrm{s}}) \, \mathrm{d}A. \tag{4.5}$$

(As usual, the time dependence that would generally appear in the argument of λ^{s} has been explicitly suppressed.) The field λ^{s} is a *macroscale* field, one whose functional dependence upon the volumetric microscale field λ can be established from (4.4) as follows.

A differential volume element $\mathrm{d}V$ can be represented by the expression (cf. (A 24))

$$\mathrm{d}V = \mathrm{d}*A \, \mathrm{d}n, \tag{4.6}$$

with $\mathrm{d}*A$ a differential areal element on a q^3-coordinate surface. Upon using the projection relation (2.16), this becomes

$$\mathrm{d}V = *M \, \mathrm{d}A \, \mathrm{d}n \tag{4.7}$$

in terms of the projected differential areal element dA lying on the interfacial parent surface $n = 0$. Use of the above relation permits a separation of the volume integral in (4.4) into a two-fold integration: (i) along the q^3-coordinate curve; and (ii) over the parent surface. Explicitly,

$$\int_V (\lambda - \bar{\lambda}) \, dV = \int_A dA \int_{n=-*L_2}^{n=*L_1} *M(\boldsymbol{x}_s, n) \left[\lambda(\boldsymbol{x}_s, n) - \bar{\lambda}(\boldsymbol{x}_s, \bar{n})\right] dn. \qquad (4.8)$$

Here, the lengths $*L_1(\boldsymbol{x}_s)$ and $*L_2(\boldsymbol{x}_s)$ respectively represent the distances separating the parent surface A from the two end caps $*A_1$ and $*A_2$, such distances being measured along q^3-coordinate curves (see figure 4). Recognizing that A can be chosen arbitrarily, substitute (4.8) into (4.4) and use the definition (4.5) for $\boldsymbol{\lambda}^s$, so as to obtain

$$\boldsymbol{\lambda}^s(\boldsymbol{x}_s) = \lim_{\epsilon \to 0} \int_{n=-*L_2}^{n=*L_1} *M(\boldsymbol{x}_s, n) \left[\lambda(\boldsymbol{x}_s, n) - \bar{\lambda}(\boldsymbol{x}_s, \bar{n})\right] dn. \qquad (4.9)$$

This expression may be simplified by decomposing the above integral into the sum of three separate integrals, corresponding to respective contributions from the two outer regions and the inner interfacial transition region:

$$\boldsymbol{\lambda}^s(\boldsymbol{x}_s) = \lim_{\epsilon \to 0} \left[\int_{n=*I_1}^{n=*L_1} *M(\lambda - \bar{\lambda}_1) \, dn + \int_{n=-*L_2}^{n=-*I_2} *M(\lambda - \bar{\lambda}_2) \, dn + \int_{n=-*I_2}^{n=*I_1} *M(\lambda - \bar{\lambda}) \, dn \right]. \qquad (4.10)$$

Here, the lengths $*I_1$ and $*I_2$ represent 'distances' separating the coordinate parent surface from the respective upper and lower intermediate regions, such distances being measured along q^3-coordinate curves. The precise choice of these lengths is immaterial (as is equally true of $*L_1$ and $*L_2$) so long as each lies within the respective domains of validity of both the inner and outer expansions (i.e. they both lie within the intermediate regions above and below the parent surface).

Within the upper outer region, $*I_1 \leqslant n \leqslant *L_1$, the representation (3.10*a*) is applicable. This, together with the requirement (3.12) imposed upon $\bar{\lambda}_{1R}$, reduces the first integral in (4.10) to the form

$$\lim_{\epsilon \to 0} \left[\int_{n=*I_1}^{n=*L_1} *M(\lambda - \bar{\lambda}_1) \, dn \right] = \lim_{\epsilon \to 0} \left[\int_{n=*I_1}^{n=*L_1} *M \bar{\lambda}_{1R} \, dn \right] = \boldsymbol{0}. \qquad (4.11)$$

The final equality in the above expression is obtained by recognizing that $*M$ remains finite as $\epsilon \to 0$, since $*M$ is independent of ϵ within each of the outer regions. Similarly, in the lower outer region, $*I_2 \leqslant -n \leqslant *L_2$, we obtain

$$\lim_{\epsilon \to 0} \left[\int_{n=-*L_2}^{n=-*I_2} *M(\lambda - \bar{\lambda}_2) \, dn \right] = \lim_{\epsilon \to 0} \left[\int_{n=-*L_2}^{n=-*I_2} *M \bar{\lambda}_{2R} \, dn \right] = \boldsymbol{0}. \qquad (4.12)$$

Within the inner region, $-*I_2 \leqslant n \leqslant *I_1$, equation (3.6) can be used to represent λ, thereby yielding

$$\lim_{\epsilon \to 0} \left[\int_{n=-*I_2}^{n=*I_1} *M(\lambda - \bar{\lambda}) \, dn \right] = \lim_{\epsilon \to 0} \left[\int_{n=-*I_2}^{n=*I_1} *M(\tilde{\lambda} - \bar{\lambda}) \, dn + \int_{n=-*I_2}^{n=*I_1} *M \tilde{\lambda}_R \, dn \right] \qquad (4.13)$$

for the last integral in (4.10). The condition (3.8) imposed upon $\tilde{\lambda}_{\rm R}$ assures that

$$\lim_{\epsilon \to 0}\left[\int_{n=-*I_2}^{n=*I_1} *M\,\tilde{\lambda}_{\rm R}\,{\rm d}n \right] = 0. \tag{4.14}$$

Use of (3.1)–(3.3), (3.17), (3.25a), and (3.26a) permits one to write

$$\lim_{\epsilon \to 0}\left\{ \int_{n=-*I_2}^{n=*I_1} *M(\boldsymbol{x}_{\rm s}, n)\,[\bar{\tilde{\lambda}}(\boldsymbol{x}_{\rm s}, \tilde{n}) - \bar{\lambda}(\boldsymbol{x}_{\rm s}, \bar{n})]\,{\rm d}n \right\}$$

$$= \lim_{\epsilon \to 0}\left\{ \epsilon L \int_{\tilde{n}=-c_2\epsilon^{r-1}}^{\tilde{n}=c_1\epsilon^{r-1}} [1 + O(\epsilon^r)]\,[\bar{\tilde{\lambda}}(\boldsymbol{x}_{\rm s}, \tilde{n}) - \bar{\lambda}(\boldsymbol{x}_{\rm s}, \bar{n} = \epsilon\tilde{n})]\,{\rm d}\tilde{n} \right\}, \tag{4.15}$$

with c_1 and c_2 positive numbers whose values may depend upon $\boldsymbol{x}_{\rm s}$, but are independent of ϵ. Passage to the limit in the latter half of (4.15) furnishes the asymptotic relation

$$\lim_{\epsilon \to 0}\left[\int_{n=-*I_2}^{n=*I_1} *M(\tilde{\lambda} - \bar{\lambda})\,{\rm d}n \right] \sim \epsilon L \int_{\tilde{n}=-\infty}^{+\infty} [\bar{\tilde{\lambda}}(\boldsymbol{x}_{\rm s}, \tilde{n}) - \bar{\lambda}(\boldsymbol{x}_{\rm s}, 0)]\,{\rm d}\tilde{n}, \tag{4.16}$$

wherein

$$\bar{\lambda}(\boldsymbol{x}_{\rm s}, 0) \overset{\rm def}{=} \begin{cases} \lim_{\bar{n} \to 0+} \bar{\lambda}_1(\boldsymbol{x}_{\rm s}, \bar{n}) & (\tilde{n} > 0), \\ \lim_{\bar{n} \to 0-} \bar{\lambda}_2(\boldsymbol{x}_{\rm s}, \bar{n}) & (\tilde{n} < 0). \end{cases} \tag{4.17}$$

Substitution of (4.11)–(4.14), and (4.16) into (4.10) thereby yields the operational definition

$$\boldsymbol{\lambda}^{\rm s}(\boldsymbol{x}_{\rm s}) \sim \epsilon L \int_{\tilde{n}=-\infty}^{+\infty} [\bar{\tilde{\lambda}}(\boldsymbol{x}_{\rm s}, \tilde{n}) - \bar{\lambda}(\boldsymbol{x}_{\rm s}, 0)]\,{\rm d}\tilde{n} \tag{4.18}$$

for the surface-excess areal density field $\boldsymbol{\lambda}^{\rm s}$ in terms the indicated quadrature of the respective inner field $\tilde{\lambda}$ and outer field limits $\bar{\lambda}(0\pm)$ of the exact volumetric density field $\boldsymbol{\lambda}(\boldsymbol{x})$ in proximity to the interface. In order for a macroscale description of the interface to be valid, the above integral must be convergent. The matching conditions (3.18) are necessary, but insufficient, for convergence. Hereafter, we will assume that the surface-excess areal densities defined by (4.18) exist.

A similar expression for the surface-excess lineal flux density field $\boldsymbol{\varphi}^{\rm s}$ can be derived as follows from the continuous, microscale, areal flux density field $\boldsymbol{\varphi}$ of the extensive property $\mathscr{P}$. The total efflux, $\boldsymbol{\Phi}$, of $\mathscr{P}$ through the bounding surface ∂V of the surface-fixed control volume V is given by the expression

$$\boldsymbol{\Phi} \overset{\rm def}{=} \int_{\partial V} {\rm d}\boldsymbol{S} \cdot \boldsymbol{\varphi}, \tag{4.19}$$

where ${\rm d}\boldsymbol{S}$ is a directed surface element on ∂V, possessing the direction of the outward-drawn normal to ∂V (see figure 4). A macroscale experimentalist whose instruments traverse the volume V will, however, resolve and hence observe only the macroscale field $\bar{\boldsymbol{\varphi}}$ (cf. (4.1)), thus concluding that the total efflux, $\bar{\boldsymbol{\Phi}}$ of $\mathscr{P}$ through the surface of the control volume is given rather by

$$\bar{\boldsymbol{\Phi}} = \int_{\partial V} {\rm d}\boldsymbol{S} \cdot \bar{\boldsymbol{\varphi}}. \tag{4.20}$$

Such a macroscale observer will suppose that any discrepancy existing between the exact and macroscale fluxes $\boldsymbol{\Phi}$ and $\bar{\boldsymbol{\Phi}}$ is caused by an efflux of $\mathscr{P}$ *along* the interface, thereby obtaining

$$\boldsymbol{\Phi}^{\mathrm{s}} \stackrel{\text{def}}{=} \lim_{\epsilon \to 0} (\boldsymbol{\Phi} - \bar{\boldsymbol{\Phi}}) \equiv \lim_{\epsilon \to 0} \int_{\partial V} \mathrm{d}\boldsymbol{S} \cdot [\boldsymbol{\varphi}(\boldsymbol{x}_{\mathrm{s}}, n) - \bar{\boldsymbol{\varphi}}(\boldsymbol{x}_{\mathrm{s}}, \bar{n})] \tag{4.21}$$

for the surface-excess efflux, $\boldsymbol{\Phi}^{\mathrm{s}}$, of $\mathscr{P}$ through the closed curve ∂A. Here again, we are formally identifying the mathematical parent surface with the physical macroscale interface in the $\epsilon \to 0$ limit. A continuous, surface-excess lineal flux-density field $\boldsymbol{\varphi}^{\mathrm{s}}$ can now be defined at every point $\boldsymbol{x}_{\mathrm{s}}$ (and, of course, every time t) by the expression

$$\boldsymbol{\Phi}^{\mathrm{s}} \stackrel{\text{def}}{=} \int_{\partial A} \mathrm{d}\boldsymbol{C} \cdot \boldsymbol{\varphi}^{\mathrm{s}}(\boldsymbol{x}_{\mathrm{s}}), \tag{4.22}$$

where $\mathrm{d}\boldsymbol{C} = \boldsymbol{m}\,\mathrm{d}C$ is a directed line element on ∂A possessing the direction of the outward-drawn normal to A (see figure 4). The field $\boldsymbol{\varphi}^{\mathrm{s}}$ is a macroscale field, one whose functional dependence upon the three-dimensional areal flux $\boldsymbol{\varphi}$ can be established from (4.21) as follows.

A differential element of surface $\mathrm{d}\boldsymbol{S}$ lying upon the sides of the control volume can be represented as (cf. (A 28))

$$\mathrm{d}\boldsymbol{S} = {}^{*}\boldsymbol{m}\,\mathrm{d}{}^{*}C\,\mathrm{d}n, \tag{4.23}$$

with $\mathrm{d}{}^{*}C$ a differential lineal element lying on the q^3-coordinate surface, and ${}^{*}\boldsymbol{m}$ the unit vector normal to the curve $\mathrm{d}{}^{*}C$ and lying simultaneously in the tangent plane to the q^3-coordinate surface (see figure 3). Use of the projection relation (2.18) yields

$$\mathrm{d}\boldsymbol{S} = {}^{*}\boldsymbol{m}\,{}^{*}N\,\mathrm{d}C\,\mathrm{d}n \tag{4.24}$$

in terms of the projected differential lineal element $\mathrm{d}C$ lying on the parent surface $n = 0$. The integral in (4.21) can be separated into two areal integrals over the end caps ${}^{*}A_1$ and ${}^{*}A_2$, together with an integral over the lateral q^3-coordinate curve envelope. Use of (4.24) allows this latter integral to be partitioned into an integration along the q^3-coordinate curve, followed by an integration along the curve ∂A. Performing these respective operations gives

$$\int_{\partial V} \mathrm{d}\boldsymbol{S} \cdot (\boldsymbol{\varphi} - \bar{\boldsymbol{\varphi}}) = \int_{\partial A} \mathrm{d}C \int_{n=-{}^{*}L_2}^{n={}^{*}L_1} {}^{*}N(\boldsymbol{x}_{\mathrm{s}}, n)\,{}^{*}\boldsymbol{m} \cdot [\boldsymbol{\varphi}(\boldsymbol{x}_{\mathrm{s}}, n) - \bar{\boldsymbol{\varphi}}(\boldsymbol{x}_{\mathrm{s}}, \bar{n})]\,\mathrm{d}n$$

$$+ \int_{{}^{*}A_1} \mathrm{d}{}^{*}A\,{}^{*}\boldsymbol{n} \cdot (\boldsymbol{\varphi} - \bar{\boldsymbol{\varphi}}_1) - \int_{{}^{*}A_2} \mathrm{d}{}^{*}A\,{}^{*}\boldsymbol{n} \cdot (\boldsymbol{\varphi} - \bar{\boldsymbol{\varphi}}_2). \tag{4.25}$$

Since ${}^{*}A_1$ and ${}^{*}A_2$ lie respectively within the upper and lower outer regions, (3.10) can be used to represent $\boldsymbol{\varphi}$ in the latter two integrals appearing above. This fact, in conjunction with the requirement (3.12) imposed upon $\bar{\boldsymbol{\varphi}}_{\alpha\mathrm{R}}$, yields

$$\lim_{\epsilon \to 0} \int_{{}^{*}A_\alpha} \mathrm{d}{}^{*}A\,{}^{*}\boldsymbol{n} \cdot (\boldsymbol{\varphi} - \bar{\boldsymbol{\varphi}}_\alpha) = \lim_{\epsilon \to 0} \int_{{}^{*}A_\alpha} \mathrm{d}{}^{*}A\,{}^{*}\boldsymbol{n} \cdot \bar{\boldsymbol{\varphi}}_{\alpha\mathrm{R}} = \boldsymbol{0} \quad (\alpha = 1, 2). \tag{4.26}$$

Upon recognizing that A may be chosen arbitrarily, subsequent substitution of (4.25) and (4.26) into (4.21) and utilization of the definition (4.22) for $\boldsymbol{\varphi}^{\mathrm{s}}$ eventually yields

$$\boldsymbol{m} \cdot \boldsymbol{\varphi}^{\mathrm{s}}(\boldsymbol{x}_{\mathrm{s}}) = \lim_{\epsilon \to 0} \int_{n=-{}^{*}L_2}^{n={}^{*}L_1} {}^{*}N(\boldsymbol{x}_{\mathrm{s}}, n)\,{}^{*}\boldsymbol{m} \cdot [\boldsymbol{\varphi}(\boldsymbol{x}_{\mathrm{s}}, n) - \bar{\boldsymbol{\varphi}}(\boldsymbol{x}_{\mathrm{s}}, \bar{n})]\,\mathrm{d}n. \tag{4.27}$$

The preceding expression can be decomposed into three separate contributions, corresponding to respective integrations over the two outer regions and the inner interfacial transition region; explicitly,

$$\boldsymbol{m}\cdot\boldsymbol{\varphi}^{\mathrm{s}}(\boldsymbol{x}_{\mathrm{s}}) = \lim_{\epsilon\to 0}\left[\int_{n=*I_1}^{n=*L_1} *N^*\boldsymbol{m}\cdot(\boldsymbol{\varphi}-\bar{\boldsymbol{\varphi}}_1)\,\mathrm{d}n + \int_{n=-*L_2}^{n=-*I_2} *N^*\boldsymbol{m}\cdot(\boldsymbol{\varphi}-\bar{\boldsymbol{\varphi}}_2)\,\mathrm{d}n \right.$$
$$\left. + \int_{n=-*I_2}^{n=*I_1} *N^*\boldsymbol{m}\cdot(\boldsymbol{\varphi}-\bar{\boldsymbol{\varphi}})\,\mathrm{d}n\right]. \quad (4.28)$$

Equation (3.10a) may be used to represent $\boldsymbol{\varphi}$ within the upper outer region. This representation, together with the requirement (3.12) demanded of $\bar{\boldsymbol{\varphi}}_{1\mathrm{R}}$, allows the first integral appearing in (4.28) to be written as

$$\lim_{\epsilon\to 0}\left[\int_{n=*I_1}^{n=*L_1} *N^*\boldsymbol{m}\cdot(\boldsymbol{\varphi}-\bar{\boldsymbol{\varphi}}_1)\,\mathrm{d}n\right] = \lim_{\epsilon\to 0}\left[\int_{n=*I_1}^{n=*L_1} *N^*\boldsymbol{m}\cdot\bar{\boldsymbol{\varphi}}_{1\mathrm{R}}\,\mathrm{d}n\right] = \boldsymbol{0}. \quad (4.29)$$

In obtaining the final equality in the preceding expression, it has been recognized that $*N$ remains finite as $\epsilon\to 0$, since $*N$ is independent of ϵ within the two outer regions. Similarly, upon using (3.10b) and (3.12), the second integral in (4.28) adopts the form

$$\lim_{\epsilon\to 0}\left[\int_{n=-*L_2}^{n=-*I_2} *N^*\boldsymbol{m}\cdot(\boldsymbol{\varphi}-\bar{\boldsymbol{\varphi}}_2)\,\mathrm{d}n\right] = \lim_{\epsilon\to 0}\left[\int_{n=-*L_2}^{n=-*I_2} *N^*\boldsymbol{m}\cdot\bar{\boldsymbol{\varphi}}_{2\mathrm{R}}\,\mathrm{d}n\right] = \boldsymbol{0}. \quad (4.30)$$

Equation (3.6) can be used to represent $\boldsymbol{\varphi}$ within the inner region, thereby obtaining

$$\lim_{\epsilon\to 0}\left[\int_{n=-*I_2}^{n=*I_1} *N^*\boldsymbol{m}\cdot(\boldsymbol{\varphi}-\bar{\boldsymbol{\varphi}})\,\mathrm{d}n\right]$$
$$= \lim_{\epsilon\to 0}\left[\int_{n=-*I_2}^{n=*I_1} *N^*\boldsymbol{m}\cdot(\tilde{\boldsymbol{\varphi}}-\bar{\boldsymbol{\varphi}})\,\mathrm{d}n + \int_{n=-*I_2}^{n=*I_1} *N^*\boldsymbol{m}\cdot\tilde{\boldsymbol{\varphi}}_{\mathrm{R}}\,\mathrm{d}n\right] \quad (4.31)$$

for the last integral in (4.28). The condition (3.8) required of $\tilde{\boldsymbol{\varphi}}_{\mathrm{R}}$ assures that

$$\lim_{\epsilon\to 0}\left[\int_{n=-*I_2}^{n=*I_1} *N^*\boldsymbol{m}\cdot\tilde{\boldsymbol{\varphi}}_{\mathrm{R}}\,\mathrm{d}n\right] = \boldsymbol{0}. \quad (4.32)$$

Jointly, (3.1)–(3.3), (3.17), (3.25b), (3.26b), (3.28), and (3.29) permit one to write

$$\lim_{\epsilon\to 0}\left\{\int_{n=-*I_2}^{n=*I_1} *N(\boldsymbol{x}_{\mathrm{s}},n)\,{}^*\boldsymbol{m}(\boldsymbol{x}_{\mathrm{s}},n)\cdot[\tilde{\boldsymbol{\varphi}}(\boldsymbol{x}_{\mathrm{s}},\tilde{n})-\bar{\boldsymbol{\varphi}}(\boldsymbol{x}_{\mathrm{s}},\bar{n})]\,\mathrm{d}n\right\}$$
$$= \lim_{\epsilon\to 0}\left\{\epsilon L\int_{\tilde{n}=-c_2\epsilon^{r-1}}^{\tilde{n}=c_1\epsilon^{r-1}} [1+O(\epsilon^r)]\,[\boldsymbol{m}+O(\epsilon^r)]\cdot[\tilde{\boldsymbol{\varphi}}(\boldsymbol{x}_{\mathrm{s}},\tilde{n})-\bar{\boldsymbol{\varphi}}(\boldsymbol{x}_{\mathrm{s}},\bar{n}=\epsilon\tilde{n})]\,\mathrm{d}\tilde{n}\right\}. \quad (4.33)$$

Passage to the limit in the right-hand side of the above equation thereby produces the relation

$$\lim_{\epsilon\to 0}\left[\int_{n=-*I_2}^{n=*I_1} *N^*\boldsymbol{m}\cdot(\tilde{\boldsymbol{\varphi}}-\bar{\boldsymbol{\varphi}})\,\mathrm{d}n\right] \sim \epsilon L\int_{\tilde{n}=-\infty}^{+\infty} \boldsymbol{m}\cdot[\tilde{\boldsymbol{\varphi}}(\boldsymbol{x}_{\mathrm{s}},\tilde{n})-\bar{\boldsymbol{\varphi}}(\boldsymbol{x}_{\mathrm{s}},0)]\,\mathrm{d}\tilde{n}, \quad (4.34)$$

in which the notation of (4.17) (with $\boldsymbol{\lambda}\equiv\boldsymbol{\varphi}$) has been used.

Introduce (4.29)–(4.32), and (4.34) into (4.28) to obtain

$$\boldsymbol{m} \cdot \boldsymbol{\varphi}^{\mathrm{s}}(\boldsymbol{x}_{\mathrm{s}}) \sim \epsilon L \int_{\tilde{n}=-\infty}^{+\infty} \boldsymbol{m} \cdot [\tilde{\boldsymbol{\varphi}}(\boldsymbol{x}_{\mathrm{s}}, \tilde{n}) - \bar{\boldsymbol{\varphi}}(\boldsymbol{x}_{\mathrm{s}}, 0)] \, \mathrm{d}\tilde{n}. \tag{4.35}$$

Use of the identity $\boldsymbol{m} = \boldsymbol{m} \cdot \boldsymbol{I}_{\mathrm{s}}$ yields the operational definition†

$$\boldsymbol{\varphi}^{\mathrm{s}}(\boldsymbol{x}_{\mathrm{s}}) \sim \epsilon L \int_{\tilde{n}=-\infty}^{+\infty} \boldsymbol{I}_{\mathrm{s}} \cdot [\tilde{\boldsymbol{\varphi}}(\boldsymbol{x}_{\mathrm{s}}, \tilde{n}) - \bar{\boldsymbol{\varphi}}(\boldsymbol{x}_{\mathrm{s}}, 0)] \, \mathrm{d}\tilde{n}, \tag{4.36}$$

for the surface-excess lineal flux density field $\boldsymbol{\varphi}^{\mathrm{s}}$ in terms of the inner and outer limits of the microscale areal density field $\boldsymbol{\varphi}(\boldsymbol{x})$. This integral must be convergent in order for a macroscale description of the interface to the valid. Similarly to (4.18), it will hereafter be assumed that the surface-excess flux densities defined by (4.36) exist.

The respective integral expressions (4.18) and (4.36) for the surface-excess density fields $\boldsymbol{\lambda}^{\mathrm{s}}$ and $\boldsymbol{\varphi}^{\mathrm{s}}$ are each multiplied by the smaller parameter ϵ. Thus, except for those situations in which the three-dimensional microscale continuum fields $\boldsymbol{\lambda}$ or $\boldsymbol{\varphi}$ attain large values, of $O(\epsilon^{-1})$, within the interfacial transition region, these surface-excess quantities will generally be vanishingly small. Large values of $\boldsymbol{\lambda}$ or $\boldsymbol{\varphi}$ within the interfacial transition region may be expected to exist whenever surface-active substances are adsorbed at the interface. Thus, the surface-excess densities $\boldsymbol{\lambda}^{\mathrm{s}}$ and $\boldsymbol{\varphi}^{\mathrm{s}}$ may generally be expected to be sensible when the interface contains adsorbed surfactants. Section 8 discusses these issues in more detail.

5. Generic conservation equations

Let $\boldsymbol{\psi} = \boldsymbol{\psi}(\boldsymbol{x}, t)$, which may be a scalar, vector, or tensor field, represent the generic, intensive, microscale volumetric density of some extensive physical property $\mathscr{P}$ (e.g. mass, linear momentum, etc.) of the continuum. The total amount, $\boldsymbol{\Psi}$, of $\mathscr{P}$ instantaneously contained within a moving and deforming surface-fixed control volume V (cf. figure 4) is given by (4.2) (with the choice $\boldsymbol{\lambda} \equiv \boldsymbol{\psi}$). Here, the control volume V is not necessarily constrained to straddle the interfacial transition region, as it was for the case of determining surface-excess quantities.

The generic 'conservation' (balance) equation for the total amount of $\mathscr{P}$ contained within V is given by the expression (Moeckel 1975)

$$\mathrm{d}\boldsymbol{\Psi}/\mathrm{d}t + \boldsymbol{\Phi} = \boldsymbol{\Pi} + \boldsymbol{Z}, \tag{5.1}$$

where $\boldsymbol{\Phi}$ represents the total extensive efflux (per unit time) of $\mathscr{P}$ out of V through the bounding surface ∂V of the control volume, $\boldsymbol{\Pi}$ is the time-rate of production of

---

† Since the arbitrary vector $\boldsymbol{m}$ lies only in the tangent plane, the actual solution of (4.35) is

$$\boldsymbol{\varphi}^{\mathrm{s}}(\boldsymbol{x}_{\mathrm{s}}) \sim \epsilon L \int_{\tilde{n}=-\infty}^{+\infty} [\tilde{\boldsymbol{\varphi}}(\boldsymbol{x}_{\mathrm{s}}, \tilde{n}) - \bar{\boldsymbol{\varphi}}(\boldsymbol{x}_{\mathrm{s}}, 0)] \, \mathrm{d}\tilde{n} + \boldsymbol{n}\boldsymbol{F},$$

in which $\boldsymbol{F}$ is an arbitrary three-dimensional tensor whose rank is one less than that of $\boldsymbol{\varphi}^{\mathrm{s}}$. In subsequent applications, it is only the directional quantity $\boldsymbol{I}_{\mathrm{s}} \cdot \boldsymbol{\varphi}^{\mathrm{s}}$, rather than $\boldsymbol{\varphi}^{\mathrm{s}}$ by itself, that appears. We have anticipated this by suppressing the $\boldsymbol{n}\boldsymbol{F}$ term in the above via use of the projection operator $\boldsymbol{I}_{\mathrm{s}}$ on the left-hand side of the integrand appearing in (4.36). Note that whereas $\boldsymbol{n} \cdot \boldsymbol{\varphi}^{\mathrm{s}} = \boldsymbol{0}$ identically with the choice (4.36), this does not imply that the equation $\boldsymbol{\varphi}^{\mathrm{s}} \cdot \boldsymbol{n} = \boldsymbol{0}$ is generally true for situations in which the tensorial rank of $\boldsymbol{\varphi}$ is greater than unity.

$\mathscr{P}$ within the control volume by internal sources, and $\boldsymbol{Z}$ is the rate of supply of $\mathscr{P}$ to the interior of V via the action of external sources (see table 3 for examples). Both $\boldsymbol{\Pi}$ and $\boldsymbol{Z}$ can be expressed in terms of their respective microscale volumetric densities $\boldsymbol{\pi}$ and $\boldsymbol{\zeta}$ via (4.2). Similarly, $\boldsymbol{\Phi}$ can be expressed in terms of the corresponding microscale areal tensor flux density $\boldsymbol{\varphi}$ via (4.19). (The tensorial rank of the flux density $\boldsymbol{\varphi}$ is always one rank greater than that of the volumetric density $\boldsymbol{\psi}$ of the conserved extensive property $\mathscr{P}$ being transported.) Thus, (5.1) may be written in the form

$$\frac{\mathrm{d}}{\mathrm{d}t}\int_V \boldsymbol{\psi}\,\mathrm{d}V + \int_{\partial V}\mathrm{d}\boldsymbol{S}\cdot\boldsymbol{\varphi} = \int_V (\boldsymbol{\pi}+\boldsymbol{\zeta})\,\mathrm{d}V. \tag{5.2}$$

According to the Reynolds' transport theorem,

$$\frac{\mathrm{d}}{\mathrm{d}t}\int_V \boldsymbol{\psi}\,\mathrm{d}V = \int_V\left[\frac{\delta\boldsymbol{\psi}}{\delta t}+(\nabla\cdot {}^*\boldsymbol{u})\,\boldsymbol{\psi}\right]\mathrm{d}V. \tag{5.3}$$

(This theorem is commonly written for a *material* control volume in which the mass-average fluid velocity vector $\boldsymbol{v}$ appears in place of ${}^*\boldsymbol{u}$. However, the general proof of this theorem (Aris 1962, p. 85) does not depend upon the material nature of the control volume.)

Moreover, according to the divergence theorem,

$$\int_{\partial V}\mathrm{d}\boldsymbol{S}\cdot\boldsymbol{\varphi} = \int_V \nabla\cdot\boldsymbol{\varphi}\,\mathrm{d}V. \tag{5.4}$$

Substitute (5.3) and (5.4) into (5.2), and invoke the arbitrary nature of the control volume V together with the continuous nature of each microscale field, to obtain the fundamental generic conservation equation

$$\delta\boldsymbol{\psi}/\delta t + (\nabla\cdot {}^*\boldsymbol{u})\,\boldsymbol{\psi} + \nabla\cdot\boldsymbol{\varphi} = \boldsymbol{\pi}+\boldsymbol{\zeta} \tag{5.5}$$

governing the spatio-temporal transport of the property $\mathscr{P}$.

In general, the flux

$$\boldsymbol{\varphi} = (\boldsymbol{v}-{}^*\boldsymbol{u})\,\boldsymbol{\psi}+\boldsymbol{J}, \tag{5.6}$$

arises from two distinct physical phenomena, these respectively being the convective flux $(\boldsymbol{v}-{}^*\boldsymbol{u})\,\boldsymbol{\psi}$ and the molecular (or diffusive) flux $\boldsymbol{J}$ of the property $\mathscr{P}$ through a surface-fixed areal element. Here, $\boldsymbol{v}$ is the mass-average velocity vector of a material fluid element. Use of (5.6), together with the relation (2.23) for the time derivative expressed in terms of space-fixed coordinates, allows the generic conservation equation (5.5) to be written in the classical generic eulerian form (Bird *et al.* 1960)

$$\left(\frac{\partial\boldsymbol{\psi}}{\partial t}\right)_{\boldsymbol{x}} + \nabla\cdot(\boldsymbol{v}\boldsymbol{\psi}) + \nabla\cdot\boldsymbol{J} = \boldsymbol{\pi}+\boldsymbol{\zeta}. \tag{5.7}$$

(a) *Macroscale bulk-fluid equations*

The generic conservation equation for the macroscale volumetric density $\bar{\boldsymbol{\psi}}$ is found by taking the outer limit of (5.5):

$$\lim_{\substack{\epsilon\to 0\\ \bar{n}\,\mathrm{fixed}}}\left[\frac{\delta\boldsymbol{\psi}}{\delta t}+(\nabla\cdot {}^*\boldsymbol{u})\,\boldsymbol{\psi}+\nabla\cdot\boldsymbol{\varphi}-\boldsymbol{\pi}-\boldsymbol{\zeta}\right] = \boldsymbol{0}. \tag{5.8}$$

Substitute (3.10) and (3.15) into (5.8) and utilize the fact that since $*\boldsymbol{u}$ is a macroscale quantity (cf. (2.8)) it necessarily satisfies the condition $*\bar{\boldsymbol{u}} = *\boldsymbol{u}$. This yields

$$\left[\frac{\delta\bar{\boldsymbol{\psi}}_\alpha}{\delta t} + (\nabla\cdot *\boldsymbol{u})\,\bar{\boldsymbol{\psi}}_\alpha + \nabla\cdot\bar{\boldsymbol{\varphi}}_\alpha - \bar{\boldsymbol{\pi}}_\alpha - \bar{\boldsymbol{\zeta}}_\alpha\right]$$

$$+ \lim_{\substack{\epsilon\to 0 \\ \bar{n}\,\text{fixed}}}\left[\frac{\delta\bar{\boldsymbol{\psi}}_{\alpha R}}{\delta t} + (\nabla\cdot *\boldsymbol{u})\,\bar{\boldsymbol{\psi}}_{\alpha R} + \nabla\cdot\bar{\boldsymbol{\varphi}}_{\alpha R} - \bar{\boldsymbol{\pi}}_{\alpha R} - \bar{\boldsymbol{\zeta}}_{\alpha R}\right] = 0 \quad (\alpha = 1, 2), \quad (5.9)$$

which holds strictly only for those points lying within the outer (and intermediate) regions, namely $|\bar{n}| \geqslant O(\epsilon^r)$. However, as $\epsilon \to 0$, the preceding constraint imposed upon $\bar{n}$ reduces to $|\bar{n}| > 0$.

Further progress requires additional *physical* assumptions regarding the *mathematical* nature of the generic densities $\boldsymbol{\psi}$ and $\boldsymbol{\varphi}$ for the particular class of physical problems of interest to us here. In particular, it will be supposed that both the temporal and spatial differential operations can be interchanged with the outer limit operation such that, with use of (3.12), we obtain

$$\lim_{\substack{\epsilon\to 0 \\ \bar{n}\,\text{fixed}}}\frac{\delta\bar{\boldsymbol{\psi}}_{\alpha R}}{\delta t} = 0 \quad (\alpha = 1, 2) \tag{5.10}$$

and

$$\lim_{\substack{\epsilon\to 0 \\ \bar{n}\,\text{fixed}}}\nabla\cdot\bar{\boldsymbol{\varphi}}_{\alpha R} = 0 \quad (\alpha = 1, 2). \tag{5.11}$$

These assumptions impose no significant constraints and serve to eliminate pathological density functions. In particular, if $\bar{\boldsymbol{\lambda}}_{\alpha R}$ (with $\boldsymbol{\lambda} \equiv \boldsymbol{\psi}, \boldsymbol{\varphi}$) can be written in the form

$$\bar{\boldsymbol{\lambda}}_{\alpha R}(\boldsymbol{x}_s, \bar{n}, t; \epsilon) = \bar{f}_{\alpha 1}(\epsilon)\,\bar{\boldsymbol{\lambda}}_{\alpha R_1}(\boldsymbol{x}_s, \bar{n}, t) + \bar{f}_{\alpha 2}(\epsilon)\,\bar{\boldsymbol{\lambda}}_{\alpha R_2}(\boldsymbol{x}_s, \bar{n}, t) + \dots,$$

then (5.10) and (5.11) will hold automatically. Since rapid changes in $\boldsymbol{\lambda}$ occur only with respect to the variable $\bar{n}$, the main restriction imposed upon the continuum fields by (5.11) arises due to the constraint imposed upon the normal gradient $\partial\bar{\boldsymbol{\varphi}}_{\alpha R}/\partial\bar{n}$.

Substitution of (3.12), (5.10), and (5.11) into (5.9) gives

$$\delta\bar{\boldsymbol{\psi}}/\delta t + (\nabla\cdot *\boldsymbol{u})\,\bar{\boldsymbol{\psi}} + \nabla\cdot\bar{\boldsymbol{\varphi}} = \bar{\boldsymbol{\pi}} + \bar{\boldsymbol{\zeta}} \quad (\bar{n} \neq 0). \tag{5.12}$$

This equation is separately valid within each of the two macroscale bulk-fluid phases, $\bar{n} > 0$ and $\bar{n} < 0$, although not at the interface $\bar{n} = 0$, across which any one or more of the macroscale fields (denoted by an overbar) may be discontinuous. Application of the product relation (3.15) to (5.6) yields

$$\bar{\boldsymbol{\varphi}} = (\bar{\boldsymbol{v}} - *\boldsymbol{u})\,\bar{\boldsymbol{\psi}} + \bar{\boldsymbol{J}}. \tag{5.13}$$

Thus, the generic macroscale conservation equation governing $\bar{\boldsymbol{\psi}}$ can be written in the canonical form

$$\delta\bar{\boldsymbol{\psi}}/\delta t + (\bar{\boldsymbol{v}} - *\boldsymbol{u})\cdot\nabla\bar{\boldsymbol{\psi}} + (\nabla\cdot\bar{\boldsymbol{v}})\,\bar{\boldsymbol{\psi}} + \nabla\cdot\bar{\boldsymbol{J}} = \bar{\boldsymbol{\pi}} + \bar{\boldsymbol{\zeta}} \quad (\bar{n} \neq 0). \tag{5.14}$$

(b) *Macroscale interfacial equation*

The macroscale boundary condition imposed upon the two bulk fluids at their common interface $\bar{n} = 0$ is furnished by the interfacial conservation equation now to be derived. Consider a surface-fixed control volume V straddling the interfacial

transition region (figure 4). The generic conservation equation governing the total amount of $\mathscr{P}$ contained within such a surface-fixed control volume, as observed by a microscale observer, is given by (5.2). A macroscale observer will, however, conclude from (5.12) that the relationships

$$\frac{\mathrm{d}}{\mathrm{d}t}\int_{V_\alpha} \bar{\boldsymbol{\psi}}_\alpha\,\mathrm{d}V + \int_{\partial V_\alpha}\mathrm{d}\boldsymbol{S}\cdot\bar{\boldsymbol{\varphi}}_\alpha = \int_{V_\alpha}(\bar{\boldsymbol{\pi}}_\alpha + \bar{\boldsymbol{\zeta}}_\alpha)\,\mathrm{d}V \quad (\alpha = 1,2) \tag{5.15}$$

hold separately within the two distinct regions V_1 and V_2 (bounded externally by the closed surfaces ∂V_1 and ∂V_2 respectively). In order to establish the macroscale jump boundary condition that such an observer would impose at the interface to effect closure, the macroscale balance equations (5.15) are subtracted from the exact, microscale equation (5.2), and the macroscale limit subsequently taken; explicitly,

$$\lim_{\epsilon\to 0}\left\{\left[\frac{\mathrm{d}}{\mathrm{d}t}\int_V \boldsymbol{\psi}\,\mathrm{d}V + \int_{\partial V}\mathrm{d}\boldsymbol{S}\cdot\boldsymbol{\varphi} - \int_V(\boldsymbol{\pi}+\boldsymbol{\zeta})\,\mathrm{d}V\right]\right.$$
$$\left. -\left[\frac{\mathrm{d}}{\mathrm{d}t}\int_{V_1\oplus V_2}\bar{\boldsymbol{\psi}}\,\mathrm{d}V + \int_{\partial V_1\oplus\partial V_2}\mathrm{d}\boldsymbol{S}\cdot\bar{\boldsymbol{\varphi}} - \int_{V_1\oplus V_2}(\bar{\boldsymbol{\pi}}+\bar{\boldsymbol{\zeta}})\,\mathrm{d}V\right]\right\} = \boldsymbol{0}. \tag{5.16}$$

The preceding expression can be simplified by separately examining the comparable micro- and macroscale terms appearing in the above integrands. Towards this goal, use (4.4) and (4.5), and recall that $V_1 \oplus V_2 = V$, so as to transform the volumetric terms containing $\boldsymbol{\psi}, \boldsymbol{\pi}$, and $\boldsymbol{\zeta}$ into relations involving their surface-excess areal density counterparts, $\boldsymbol{\psi}^{\mathrm{s}}, \boldsymbol{\pi}^{\mathrm{s}}$, and $\boldsymbol{\zeta}^{\mathrm{s}}$, via the generic expression

$$\lim_{\epsilon\to 0}\int_V[\lambda(\boldsymbol{x}_{\mathrm{s}},n) - \bar{\lambda}(\boldsymbol{x}_{\mathrm{s}},\bar{n})]\,\mathrm{d}V = \int_A \lambda^{\mathrm{s}}(\boldsymbol{x}_{\mathrm{s}})\,\mathrm{d}A. \tag{5.17}$$

The applicability of the generic equation (5.17) to the function $\boldsymbol{\psi}$ depends upon the validity of the assumption

$$\lim_{\substack{\epsilon\to 0\\ \tilde{n}\,\text{fixed}}}\frac{\delta\tilde{\boldsymbol{\psi}}_{\alpha\mathrm{R}}}{\delta t} = \boldsymbol{0} \quad (\alpha = 1,2), \tag{5.18}$$

namely that the time-derivative and $\epsilon\to 0$ limit operations can be interchanged within the inner region. Upon using (4.21) and (4.22), those integrals in (5.16) containing the flux field $\boldsymbol{\varphi}$ can be written in the form

$$\lim_{\epsilon\to 0}\left[\int_{\partial V}\mathrm{d}\boldsymbol{S}\cdot\boldsymbol{\varphi}(\boldsymbol{x}_{\mathrm{s}},n) - \int_{\partial V_1\oplus\partial V_2}\mathrm{d}\boldsymbol{S}\cdot\bar{\boldsymbol{\varphi}}(\boldsymbol{x}_{\mathrm{s}},\bar{n})\right]$$
$$= \int_{\partial A}\mathrm{d}\boldsymbol{C}\cdot\boldsymbol{\varphi}^{\mathrm{s}}(\boldsymbol{x}_{\mathrm{s}}) + \int_A \mathrm{d}A\,\boldsymbol{n}\cdot[\bar{\boldsymbol{\varphi}}_1(\boldsymbol{x}_{\mathrm{s}},0) - \bar{\boldsymbol{\varphi}}_2(\boldsymbol{x}_{\mathrm{s}},0)], \tag{5.19}$$

involving the surface-excess lineal flux density $\boldsymbol{\varphi}^{\mathrm{s}}$. The last integral on the right-hand side arises because A is a subset of both ∂V_1 and ∂V_2, but not of ∂V. Use of the above results, together with the definition (3.14) of the jump discontinuity, permits (5.16) to be written as

$$\frac{\mathrm{d}}{\mathrm{d}t}\int_A \boldsymbol{\psi}^{\mathrm{s}}(\boldsymbol{x}_{\mathrm{s}})\,\mathrm{d}A + \int_{\partial A}\mathrm{d}\boldsymbol{C}\cdot\boldsymbol{\varphi}^{\mathrm{s}}(\boldsymbol{x}_{\mathrm{s}}) + \int_A \boldsymbol{n}\cdot[\![\bar{\boldsymbol{\varphi}}]\!]\,\mathrm{d}A - \int_A[\boldsymbol{\pi}^{\mathrm{s}}(\boldsymbol{x}_{\mathrm{s}}) + \boldsymbol{\zeta}^{\mathrm{s}}(\boldsymbol{x}_{\mathrm{s}})]\,\mathrm{d}A = \boldsymbol{0}. \tag{5.20}$$

According to the surface analog of Reynolds' transport theorem (Eliassen 1963),

$$\frac{\mathrm{d}}{\mathrm{d}t}\int_A \boldsymbol{\psi}^{\mathrm{s}}\,\mathrm{d}A = \int_A\left[\frac{\delta_{\mathrm{s}}\boldsymbol{\psi}^{\mathrm{s}}}{\delta t} + (\nabla_{\mathrm{s}}\cdot\boldsymbol{u})\,\boldsymbol{\psi}^{\mathrm{s}}\right]\mathrm{d}A. \tag{5.21}$$

Moreover, according to the divergence theorem for a surface (Eliassen 1963; Aris 1962),

$$\int_{\partial A}\mathrm{d}\boldsymbol{C}\cdot\boldsymbol{\varphi}^{\mathrm{s}} = \int_A \nabla_{\mathrm{s}}\cdot(\boldsymbol{I}_{\mathrm{s}}\cdot\boldsymbol{\varphi}^{\mathrm{s}})\,\mathrm{d}A. \tag{5.22}$$

(Equation (5.22) is a generic equation that applies for any tensor field $\boldsymbol{\varphi}^{\mathrm{s}}$, rather than being limited to the quantity $\boldsymbol{\varphi}^{\mathrm{s}}$ defined in (4.36). However, since (5.22) will only be used for the specific integrand $\boldsymbol{\varphi}^{\mathrm{s}}$ defined in (4.36), one could strictly suppress the $\boldsymbol{I}_{\mathrm{s}}$ appearing in the right-hand side of (5.22) as being redundant; that is, $\boldsymbol{\varphi}^{\mathrm{s}} = \boldsymbol{I}_{\mathrm{s}}\cdot\boldsymbol{\varphi}^{\mathrm{s}}$. Nevertheless, this redundancy will be retained.)

As the choice of the areal domain A is arbitrary, introduction of (5.21) and (5.22) into (5.20) furnishes the pointwise interfacial conservation equation

$$\delta_{\mathrm{s}}\boldsymbol{\psi}^{\mathrm{s}}/\delta t + (\nabla_{\mathrm{s}}\cdot\boldsymbol{u})\,\boldsymbol{\psi}^{\mathrm{s}} + \nabla_{\mathrm{s}}\cdot(\boldsymbol{I}_{\mathrm{s}}\cdot\boldsymbol{\varphi}^{\mathrm{s}}) - \boldsymbol{\pi}^{\mathrm{s}} - \boldsymbol{\zeta}^{\mathrm{s}} = -\boldsymbol{n}\cdot[\![\bar{\boldsymbol{\varphi}}]\!], \tag{5.23}$$

valid at every point $\boldsymbol{x}_{\mathrm{s}}$ of the two-dimensional macroscale interface, located at $\bar{n} = 0$. This equation, which relates the surface-excess density fields on the left to the 'jump' (3.14) in the generally discontinuous macroscale bulk-fluid areal flux density $\bar{\boldsymbol{\varphi}}$ across the interface, constitutes the interfacial boundary condition imposed upon $\bar{\boldsymbol{\varphi}}$ at the (non-material) macroscale interface, $\bar{n} = 0$. All fields appearing in (5.23) are *macroscale* fields; thus, this interfacial equation is to be understood as describing strictly macroscale phenomena, in the same sense (and at the same macroscale level of description) as (5.12).

An alternate form of (5.23) can be developed in light of the general expression (5.6) for $\boldsymbol{\varphi}$. Application of the product relation (3.16), together with the expression (3.34) for $^*\tilde{\boldsymbol{u}}$, permits (5.6) to be written as

$$\tilde{\boldsymbol{\varphi}} = (\tilde{\boldsymbol{v}} - \boldsymbol{u})\,\tilde{\boldsymbol{\psi}} + \tilde{\boldsymbol{J}}. \tag{5.24}$$

Substitute this expression, together with (5.13), into (4.36) and use (3.34) for $^*\bar{\boldsymbol{u}}$ to obtain

$$\boldsymbol{I}_{\mathrm{s}}\cdot\boldsymbol{\varphi}^{\mathrm{s}} = (\boldsymbol{I}_{\mathrm{s}}\cdot v\psi)^{\mathrm{s}} - \boldsymbol{I}_{\mathrm{s}}\cdot\boldsymbol{u}\boldsymbol{\psi}^{\mathrm{s}} + \boldsymbol{I}_{\mathrm{s}}\cdot\boldsymbol{J}^{\mathrm{s}}. \tag{5.25}$$

Use of this relation in (5.23) yields the canonical form

$$\frac{\delta_{\mathrm{s}}\boldsymbol{\psi}^{\mathrm{s}}}{\delta t} - \boldsymbol{u}\cdot\nabla_{\mathrm{s}}\boldsymbol{\psi}^{\mathrm{s}} - 2H\boldsymbol{n}\cdot\boldsymbol{u}\boldsymbol{\psi}^{\mathrm{s}} + \nabla_{\mathrm{s}}\cdot(\boldsymbol{I}_{\mathrm{s}}\cdot v\psi)^{\mathrm{s}} + \nabla_{\mathrm{s}}\cdot(\boldsymbol{I}_{\mathrm{s}}\cdot\boldsymbol{J}^{\mathrm{s}}) - \boldsymbol{\pi}^{\mathrm{s}} - \boldsymbol{\zeta}^{\mathrm{s}} = -\boldsymbol{n}\cdot[\![(\bar{\boldsymbol{v}} - \boldsymbol{u})\,\bar{\boldsymbol{\psi}} + \bar{\boldsymbol{J}}]\!] \tag{5.26}$$

of the generic conservation equation governing interfacial transport, applicable to both material and nonmaterial interfaces. In this equation, $H = -\frac{1}{2}\nabla_{\mathrm{s}}\cdot\boldsymbol{n}$ is the mean curvature of the macroscale interface.

For material interfaces, the mass-average velocity vector $\boldsymbol{v}$ satisfies the relation

$$\boldsymbol{n}\cdot\lim_{\bar{n}\to 0+}\bar{\boldsymbol{v}}_1(\boldsymbol{x}_{\mathrm{s}},\bar{n}) = \boldsymbol{n}\cdot\lim_{\bar{n}\to 0-}\bar{\boldsymbol{v}}_2(\boldsymbol{x}_{\mathrm{s}},\bar{n}) = \boldsymbol{n}\cdot\boldsymbol{u}, \tag{5.27}$$

whence only the macroscale molecular flux term $\bar{\boldsymbol{J}}$ will appear in the jump boundary condition.

Table 3. *Identification of generic fields*

(In this table, ρ = mass density, v = mass-average velocity vector, P = stress dyadic, F = external body-force density vector, a = internal angular momentum pseudovector, C = couple stress pseudodyadic, G = external body-couple density pseudovector, ρ_i = species mass density, j_i = species diffusive mass flux vector (measured relative to v), and R_i = chemical reaction rate of production of species i.)

physical quantity conserved, $\mathscr{P}$	volumetric property density ψ	areal molecular flux, J	volumetric internal production rate, π	volumetric external supply rate, ζ
mass	ρ	0	0	0
linear momentum	ρv	$-P$	0	F
angular momentum	$x \times (\rho v) + \rho a$	$P \times x - C$	0	$x \times F + G$
mass of species i	ρ_i	j_i	R_i	0

(c) *Specific physical choices for the density functions*

In order to model any specific physical system, the extensive physical property to be considered (e.g. mass, momentum, species mass, etc.), as well as the appropriate continuum density fields, represented by the abstract generic symbols in our conservation equations, must be identified. For several physical situations, table 3 provides an identification of the generic mathematical field quantities appearing in the pertinent conservation equations.

Having identified the physical microscale density fields, constitutive equations for J, π, and ζ are needed for each physical transport process. These microscale relations will ultimately give rise to corresponding *macroscale* conservation and constitutive equations governing the respective bulk-phase and interfacial transport processes. The macroscale conservation equations for the two, outer, bulk-fluid regions are determined by (5.14), with macroscale densities defined in (3.11). Because of the separability condition (3.15), the bulk-fluid equations will reduce to the familiar conservation and constitutive equations for three-dimensional fluids, albeit characterized by different phenomenological coefficients on either side of the interface. Owing to the familiar nature of these bulk-fluid transport equations (Bird *et al.* 1960), attention need only be focused on developing the interfacial transport equations.

Equation (5.26) constitutes the generic macroscale interfacial conservation equation, with surface-excess fields determined from the underlying microscale densities via (4.18) and (4.36). The latter integral representations of these surface-excess fields ultimately furnish explicit expressions for the macroscale interfacial constitutive equations and concomitant interfacial phenomenological properties characterizing physical systems of the type described in table 3. The remainder of this paper, as well as Part II (the following paper), will be devoted to an examination of macroscale interfacial relations using the asymptotic theory provided herein.

6. Interfacial properties in the presence of interphase mass transfer

When mass transfer occurs across the interface, the concept of an interfacial (material) property necessarily becomes ambiguous in any purely macroscale description (Scriven 1960; Slattery 1964a) of the phenomenon (see the discussion in

§1). (In such classical macroscale theories, entities such as $\boldsymbol{\psi}^{\mathrm{s}}$ are regarded as primitive, axiomatic, continuum-mechanical fields possessing a physically-based existence, and hence not requiring any finer-scale interpretation; as such, these theories fail to properly distinguish between 'surface' and 'surface-excess' quantities.) This inherent ambiguity arises from the fact that the phase interface is not necessarily composed of material points. The three-dimensional microscale approach of this paper resolves this macroscale issue, since surface-excess properties are herein defined independently of the existence of material interfacial elements. However, one question still arises regarding the nature of the interfacial properties. Is it possible to reconcile the 'material' interfacial densities appearing in purely classical macroscale theories (Scriven 1960; Slattery 1964a) with the surface-excess properties derived from our underlying microscale theory for systems undergoing interphase mass transport? For example, strictly macroscale theories generally assume (by analogy with comparable three-dimensional phenomena) that the interfacial linear momentum density is identified with the product $\rho^{\mathrm{s}} V$ of the purely macroscale field variables ρ^{s} and V, where ρ^{s} is a surface mass density and V is the material (i.e. mass-average) surface-velocity vector of the fictitious surface particles. (Some of the confusion that results when a two-dimensional surface approach is used to treat systems undergoing interphase mass transport can be seen by the fact that Moeckel (1975) suggests that $\boldsymbol{n} \cdot \boldsymbol{V} \neq \boldsymbol{n} \cdot \boldsymbol{u}$ in some circumstances, whereas Deemer & Slattery (1978) assume that $\boldsymbol{n} \cdot \boldsymbol{V} = \boldsymbol{n} \cdot \boldsymbol{u}$ in all circumstances.)

The question of the existence of such an apparent 'material' interfacial velocity V in systems undergoing interphase mass transport can be resolved by using our asymptotic theory of interfacial phenomena to establish whether the implicitly assumed fundamental relation

$$(\rho \boldsymbol{v})^{\mathrm{s}} = \rho^{\mathrm{s}} V \tag{6.1}$$

is valid and, if so, derive an appropriate expression for the macroscale interfacial vector field $V(\boldsymbol{x}_{\mathrm{s}})$ in terms of more fundamental microscale fields. To investigate the existence of such a vector field V, consider the microscale continuity equation

$$\delta \rho / \delta t + (\boldsymbol{v} - {}^{*}\boldsymbol{u}) \cdot \nabla \rho + (\nabla \cdot \boldsymbol{v}) \rho = 0, \tag{6.2}$$

derived from (5.5) with the conserved property in table 3 being the mass. Within the interfacial transition region, the above relation may be written in the form

$$(\boldsymbol{v} - {}^{*}\boldsymbol{u}) \cdot {}^{*}\boldsymbol{n} \frac{\partial \rho}{\partial \tilde{n}} + {}^{*}\boldsymbol{n} \cdot \frac{\partial \boldsymbol{v}}{\partial \tilde{n}} \rho + \epsilon L \left[\frac{\delta \rho}{\delta t} + (\boldsymbol{v} - {}^{*}\boldsymbol{u}) \cdot {}^{*}\nabla_{\mathrm{s}} \rho + ({}^{*}\nabla_{\mathrm{s}} \cdot \boldsymbol{v}) \rho \right] = 0. \tag{6.3}$$

Suppose that the two bulk fluid phases possess different bulk densities $\bar{\rho}_1$ and $\bar{\rho}_2$. In such situations, the microscale mass density field ρ will vary sharply within the interfacial region in the direction normal to the macroscale interface; thus, the scaling

$$\left(\frac{1}{\bar{\rho}} \right) \frac{\partial \rho}{\partial \tilde{n}} \equiv O(1) \tag{6.4}$$

is appropriate within the interfacial transition region. It will further be assumed that tangential gradients, if any, of the microscale fields ρ and $\boldsymbol{v}$ are everywhere of macroscale order; explicitly,

$$(L/\bar{\rho}) {}^{*}\nabla_{\mathrm{s}} \rho = O(1), \quad \text{and} \quad (L/U) {}^{*}\nabla_{\mathrm{s}} \boldsymbol{v} = O(1). \tag{6.5a, b}$$

The above assumptions encompass most conceivable nonpathological physical situations and, hence, do not unduly restrict the physical applicability of our final results. As a consequence of the preceding assumptions, it follows from (6.3) that

$$\left(\frac{1}{U}\right)\frac{\partial \boldsymbol{v}}{\partial \tilde{n}} \equiv O(1) \tag{6.6}$$

within the interfacial transition region. Recourse to (2.8), (2.5), and (2.14) yields

$$\left(\frac{1}{U}\right)\frac{\partial^* \boldsymbol{u}}{\partial \tilde{n}} = \left(\frac{\epsilon}{U}\right)\frac{\partial^* \boldsymbol{u}}{\partial \overline{n}} = O(\epsilon), \quad \text{and} \quad \frac{\partial^* \boldsymbol{n}}{\partial \tilde{n}} = \epsilon\frac{\partial^* \boldsymbol{n}}{\partial \overline{n}} = O(\epsilon). \tag{6.7 a, b}$$

Substitution of the above order-of-magnitude relations into (6.3) furnishes the relation

$$\frac{\partial}{\partial \tilde{n}}[(\boldsymbol{v}-{}^*\boldsymbol{u})\cdot{}^*\boldsymbol{n}\,\rho] = O(\epsilon). \tag{6.8}$$

Integrate the latter expression to obtain

$$(\boldsymbol{v}-{}^*\boldsymbol{u})\cdot{}^*\boldsymbol{n}\rho = c(\boldsymbol{x}_{\mathrm{s}})+O(\epsilon^r), \tag{6.9}$$

valid within the interfacial transition region. Here, the function $c(\boldsymbol{x}_{\mathrm{s}})$ is independent of n. Form the limit of the above equation as $\epsilon \to 0$ (with $\tilde{n}$ fixed) to obtain

$$[\tilde{\boldsymbol{v}}(\boldsymbol{x}_{\mathrm{s}},\tilde{n})-\boldsymbol{u}(\boldsymbol{x}_{\mathrm{s}})]\cdot\boldsymbol{n}(\boldsymbol{x}_{\mathrm{s}})\,\tilde{\rho}(\boldsymbol{x}_{\mathrm{s}},\tilde{n}) = c(\boldsymbol{x}_{\mathrm{s}}), \tag{6.10}$$

where (3.34) (with $^*\boldsymbol{f} \equiv {}^*\boldsymbol{u}, \, {}^*\boldsymbol{n}$) has been used. Matching conditions (3.18) thus permit us to conclude that

$$[\overline{\boldsymbol{v}}_\alpha(\boldsymbol{x}_{\mathrm{s}},0)-\boldsymbol{u}(\boldsymbol{x}_{\mathrm{s}})]\cdot\boldsymbol{n}(\boldsymbol{x}_{\mathrm{s}})\,\overline{\rho}_\alpha(\boldsymbol{x}_{\mathrm{s}},0) = c(\boldsymbol{x}_{\mathrm{s}}) \quad (\alpha = 1, 2). \tag{6.11}$$

Subtraction of the latter from (6.10) thereby yields

$$\tilde{\rho}(\tilde{n})\,\boldsymbol{n}\cdot\tilde{\boldsymbol{v}}(\tilde{n})-\overline{\rho}(0)\,\boldsymbol{n}\cdot\overline{\boldsymbol{v}}(0) = [\tilde{\rho}(\tilde{n})-\overline{\rho}(0)]\,\boldsymbol{n}\cdot\boldsymbol{u}, \tag{6.12}$$

in which the explicit dependence of the indicated arguments upon $\boldsymbol{x}_{\mathrm{s}}$ has been suppressed.

Consider those interfacial systems for which the tangential component,

$$\boldsymbol{v}_{\mathrm{s}} \equiv {}^*\boldsymbol{I}_{\mathrm{s}}\cdot\boldsymbol{v}, \tag{6.13}$$

of the microscale velocity vector is a macroscale quantity, thus obeying the scaling relation

$$\left(\frac{1}{U}\right)\frac{\partial \boldsymbol{v}_{\mathrm{s}}}{\partial \overline{n}} = O(1). \tag{6.14}$$

The above relation enables the generic proof embodied in (3.30)–(3.34) to be applied specifically to $\boldsymbol{v}_{\mathrm{s}}$ (with $^*\boldsymbol{f} \equiv \boldsymbol{v}_{\mathrm{s}}(\boldsymbol{x}_{\mathrm{s}},n)$ and $\boldsymbol{f} \equiv \boldsymbol{v}_{\mathrm{s}}(\boldsymbol{x}_{\mathrm{s}},0)$), thereby furnishing the equalities

$$\tilde{\boldsymbol{v}}_{\mathrm{s}}(\boldsymbol{x}_{\mathrm{s}},\tilde{n}) = \boldsymbol{v}_{\mathrm{s}}(\boldsymbol{x}_{\mathrm{s}},0) = \lim_{\overline{n}\to 0+}\overline{(\boldsymbol{v}_{\mathrm{s}})}_1(\boldsymbol{x}_{\mathrm{s}},\overline{n}) = \lim_{\overline{n}\to 0-}\overline{(\boldsymbol{v}_{\mathrm{s}})}_2(\boldsymbol{x}_{\mathrm{s}},\overline{n}). \tag{6.15}$$

The surface-excess linear momentum density is given by (4.18) with $\boldsymbol{\lambda} \equiv \rho\boldsymbol{v}$ as

$$(\rho\boldsymbol{v})^{\mathrm{s}} \sim \epsilon L \int_{\tilde{n}=-\infty}^{+\infty} [\widetilde{\rho\boldsymbol{v}}(\boldsymbol{x}_{\mathrm{s}},\tilde{n})-\overline{\rho\boldsymbol{v}}(\boldsymbol{x}_{\mathrm{s}},0)]\,\mathrm{d}\tilde{n}. \tag{6.16}$$

Table 4. *Definitions of important velocity fields*

symbol	definition	location in text[a]
$\boldsymbol{u} = (\partial \boldsymbol{x}_\mathrm{s}/\partial t)_{q^1,q^2}$	parent surface coordinate velocity vector: velocity of the parent surface as seen by a space-fixed observer	(2.3), figure 2
$^*\boldsymbol{u} = (\partial \boldsymbol{x}/\partial t)_{q^1,q^2,q^3}$	coordinate velocity vector: velocity of the surface-fixed coordinate system as seen by a space-fixed observer	(2.7), figure 2
$\boldsymbol{v}$	mass-average velocity vector of a material fluid element	follows (5.6)
$\boldsymbol{v}_\mathrm{s} \equiv {}^*\boldsymbol{I}_\mathrm{s}\cdot\boldsymbol{v}$	tangential component of $\boldsymbol{v}$ on coordinate surface	(6.13)
$V = \boldsymbol{v}_\mathrm{s}(0)+\boldsymbol{nn}\cdot\boldsymbol{u}$	apparent 'material' interfacial velocity vector	(6.1) and (6.19)
$\bar{\boldsymbol{v}}$	'bulk-phase' mass-average velocity vector; normal component generally discontinuous across interface	see (3.11 a, b) for generic definition

[a] The word 'location' refers to the place in the text at which the symbol is first defined or used.

Decompose $\boldsymbol{v}$ into its normal and tangential components and use (3.15), (3.16) and (3.34) ($^*\boldsymbol{f} \equiv {}^*\boldsymbol{n}$) to obtain

$$(\rho\boldsymbol{v})^\mathrm{s} \sim \epsilon L \int_{\tilde{n}=-\infty}^{+\infty} \boldsymbol{n}[\tilde{\rho}(\tilde{n})\,\boldsymbol{n}\cdot\tilde{\boldsymbol{v}}(\tilde{n}) - \bar{\rho}(0)\,\boldsymbol{n}\cdot\bar{\boldsymbol{v}}(0)]\,\mathrm{d}\tilde{n}$$

$$+\epsilon L \int_{\tilde{n}=-\infty}^{+\infty} [\tilde{\rho}(\tilde{n})\,\tilde{\boldsymbol{v}}_\mathrm{s}(\tilde{n}) - \bar{\rho}(0)\,\bar{\boldsymbol{v}}_\mathrm{s}(0)]\,\mathrm{d}\tilde{n}, \quad (6.17)$$

where, again, the explicit dependence of the arguments upon $\boldsymbol{x}_\mathrm{s}$ has been suppressed. Substitution of (6.12) and (6.15) into the above eventually yields the fundamental relation (6.1), wherein

$$\rho^\mathrm{s}(\boldsymbol{x}_\mathrm{s}) \sim \epsilon L \int_{\tilde{n}=-\infty}^{+\infty} [\tilde{\rho}(\boldsymbol{x}_\mathrm{s},\tilde{n}) - \bar{\rho}(\boldsymbol{x}_\mathrm{s},0)]\,\mathrm{d}\tilde{n} \qquad (6.18)$$

is the surface-excess mass density, defined by (4.18) with $\lambda \equiv \rho$, and

$$V(\boldsymbol{x}_\mathrm{s}) = \boldsymbol{v}_\mathrm{s}(\boldsymbol{x}_\mathrm{s},0)+\boldsymbol{n}(\boldsymbol{x}_\mathrm{s})\,\boldsymbol{n}(\boldsymbol{x}_\mathrm{s})\cdot\boldsymbol{u}(\boldsymbol{x}_\mathrm{s}) \qquad (6.19)$$

is the apparent material interfacial velocity vector. Similarly, the implicitly assumed identity

$$\boldsymbol{I}_\mathrm{s}\cdot(\rho\boldsymbol{vv})^\mathrm{s} = \boldsymbol{I}_\mathrm{s}\cdot(\rho^\mathrm{s}\,VV) \qquad (6.20)$$

for the nonlinear convective inertial term in the dynamical equations of interfacial motion may likewise be shown to be valid under the circumstances described above.

The appellation 'material interfacial velocity' applied to the vector in (6.19) is reasonably apt. Among other things, it satisfies the necessary kinematical constraint

$$\boldsymbol{n}\cdot V = \boldsymbol{n}\cdot\boldsymbol{u} \qquad (6.21)$$

imposed upon its normal component. Additionally, in the dynamical context of (6.1), V is appropriately related to the surface-excess flux of linear momentum density. Finally, this definition of V is equivalent to that obtained for material (rather than phase) interfaces.

Table 4 conveniently summarizes the various velocity fields used in the text.

Our definition (6.19) of the apparent material interfacial velocity V for systems

undergoing interphase mass transfer is equivalent to that *assumed* by Deemer & Slattery (1978). Here, however, we have been able to *prove* that such an interfacial velocity can be defined, i.e. that it exists, at least in an asymptotic sense for the conditions outlined above.

7. Physically-specific interfacial conservation equations

In this section we simplify the interfacial conservation equations for those physical properties described in table 3, based upon hypotheses which hold in most non-pathological physical situations. However, in order to keep the present contribution as broadly applicable as possible, discussion of the development of macroscale interfacial constitutive equations is postponed until Part II (following paper).

(a) Conservation of mass

With the assignations given in table 3, the interfacial conservation equation (5.26) for the mass density ($\boldsymbol{\psi} \equiv \rho$) can be written as

$$\frac{\delta_s \rho^s}{\delta t} - \boldsymbol{u} \cdot \nabla_s \rho^s - 2H\boldsymbol{n} \cdot \boldsymbol{u}\rho^s + \nabla_s \cdot (\boldsymbol{I}_s \cdot \boldsymbol{v}\rho)^s + \boldsymbol{n} \cdot [\![(\bar{\boldsymbol{v}} - \boldsymbol{u})\,\bar{\rho}]\!] = 0. \tag{7.1}$$

If (6.1) and (6.21) hold, this expression simplifies to

$$\frac{\delta_s \rho^s}{\delta t} + (\boldsymbol{V} - \boldsymbol{u}) \cdot \nabla_s \rho^s + (\nabla_s \cdot \boldsymbol{V})\rho^s + \boldsymbol{n} \cdot [\![(\bar{\boldsymbol{v}} - \boldsymbol{u})\,\bar{\rho}]\!] = 0, \tag{7.2}$$

in agreement with Deemer & Slattery (1978).

As discussed in §8, the surface-excess mass density ρ^s appearing in the above equations may normally be neglected as being of $O(\epsilon)$ since ρ is, in most physical circumstances, of $O(1)$ throughout the entire interfacial region. Thus, with

$$\rho^s = 0, \tag{7.3}$$

the surface-excess mass conservation equation (7.2) for non-material interfaces reduces to

$$\boldsymbol{n} \cdot [\![(\bar{\boldsymbol{v}} - \boldsymbol{u})\,\bar{\rho}]\!] = 0, \tag{7.4}$$

in agreement with the microscale results of (6.11). For the case of a material interface, (5.27) necessarily holds, whence (7.4) is automatically satisfied.

(b) Conservation of linear momentum

Following the identifications furnished in table 3, the interfacial conservation equation (5.26) for the linear momentum density ($\boldsymbol{\psi} \equiv \rho\boldsymbol{v}$) adopts the form

$$\frac{\delta_s (\rho\boldsymbol{v})^s}{\delta t} - \boldsymbol{u} \cdot \nabla_s (\rho\boldsymbol{v})^s - 2H\boldsymbol{n} \cdot \boldsymbol{u}(\rho\boldsymbol{v})^s + \nabla_s \cdot (\boldsymbol{I}_s \cdot \boldsymbol{vv}\rho)^s$$
$$- \nabla_s \cdot (\boldsymbol{I}_s \cdot \boldsymbol{P}^s) - \boldsymbol{F}^s + \boldsymbol{n} \cdot [\![(\bar{\boldsymbol{v}} - \boldsymbol{u})\,\bar{\rho}\,\bar{\boldsymbol{v}} - \bar{\boldsymbol{P}}]\!] = \boldsymbol{0}. \tag{7.5}$$

In circumstances for which (6.1), (6.20) and (6.21) are applicable, the above expression may be simplified with the help of (7.2) to give

$$\rho^s \left[\frac{\delta_s \boldsymbol{V}}{\delta t} + (\boldsymbol{V} - \boldsymbol{u}) \cdot \nabla_s \boldsymbol{V} \right] - \nabla_s \cdot (\boldsymbol{I}_s \cdot \boldsymbol{P}^s) - \boldsymbol{F}^s + \boldsymbol{n} \cdot [\![(\bar{\boldsymbol{v}} - \boldsymbol{u})\,(\bar{\boldsymbol{v}} - \boldsymbol{V})\,\bar{\rho}]\!] - \boldsymbol{n} \cdot [\![\bar{\boldsymbol{P}}]\!] = \boldsymbol{0}, \tag{7.6}$$

in agreement with Deemer & Slattery (1978). On the further hypothesis that (7.3) is applicable, (7.6) becomes

$$\nabla_s \cdot (\boldsymbol{I}_s \cdot \boldsymbol{P}^s) + \boldsymbol{F}^s = \boldsymbol{n} \cdot [\![(\bar{\boldsymbol{v}} - \boldsymbol{u}) \bar{\rho} \boldsymbol{v} - \bar{\boldsymbol{P}}]\!]. \tag{7.7}$$

Applications of the latter to specific dynamical problems require the specification of constitutive equations for the underlying microscale densities $\boldsymbol{F}$ and $\boldsymbol{P}$. Their specification will ultimately enable a rational derivation of the quantities $\boldsymbol{F}^s$ and $\boldsymbol{P}^s$ (as well as $\bar{\boldsymbol{P}}$).

(c) *Conservation of angular momentum*

With the choice of $\boldsymbol{\psi} \equiv \boldsymbol{x} \times (\rho \boldsymbol{v}) + \rho \boldsymbol{a}$ for the angular momentum density (table 3) and the use of (7.5) to simplify the resulting expression, (5.26) becomes

$$\frac{\delta_s (\rho \boldsymbol{a})^s}{\delta t} - \boldsymbol{u} \cdot \nabla_s (\rho \boldsymbol{a})^s - 2H \boldsymbol{n} \cdot \boldsymbol{u} (\rho \boldsymbol{a})^s + \nabla_s \cdot (\boldsymbol{I}_s \cdot \boldsymbol{v} a \rho)^s + \boldsymbol{u} \cdot \boldsymbol{n} \boldsymbol{n} \times (\rho \boldsymbol{v})^s$$

$$+ [(\boldsymbol{I}_s \cdot \boldsymbol{v}) \times \boldsymbol{v} \rho]^s - \boldsymbol{P}^s_\times - \nabla_s \cdot (\boldsymbol{I}_s \cdot \boldsymbol{C}^s) - \boldsymbol{G}^s + \boldsymbol{n} \cdot [\![(\bar{\boldsymbol{v}} - \boldsymbol{u}) \bar{\rho} \bar{\boldsymbol{a}} - \bar{\boldsymbol{C}}]\!] = \boldsymbol{0}, \tag{7.8}$$

with

$$\boldsymbol{P}^s_\times = -\boldsymbol{\varepsilon} : (\boldsymbol{I}_s \cdot \boldsymbol{P}^s) \tag{7.9}$$

the vector invariant (Gibbs & Wilson 1960) of the surface stress dyadic (which is related to the antisymmetric portion, if any, of the latter). Here, (2.3), (3.34) (with $*\boldsymbol{f} \equiv \boldsymbol{x}/L$), (A 5), and table 5 (definition of $\boldsymbol{I}_s$) have been used, together with the generic dyadic identity

$$-\nabla_s \cdot (\boldsymbol{D} \times \boldsymbol{x}_s) = \boldsymbol{x}_s \times (\nabla_s \cdot \boldsymbol{D}) + \boldsymbol{D}^s_\times, \tag{7.10}$$

in which $\boldsymbol{D}$ is an arbitrary dyadic.

In circumstances for which (6.1), (6.15), (6.20) and (6.21) hold, (7.8) may be simplified to yield

$$\frac{\delta_s (\rho \boldsymbol{a})^s}{\delta t} + (\boldsymbol{V} - \boldsymbol{u}) \cdot \nabla_s (\rho \boldsymbol{a})^s + (\nabla_s \cdot \boldsymbol{V}) (\rho \boldsymbol{a})^s - \boldsymbol{P}^s_\times$$

$$- \nabla_s \cdot (\boldsymbol{I}_s \cdot \boldsymbol{C}^s) - \boldsymbol{G}^s + \boldsymbol{n} \cdot [\![(\bar{\boldsymbol{v}} - \boldsymbol{u}) \bar{\rho} \bar{\boldsymbol{a}} - \bar{\boldsymbol{C}}]\!] = \boldsymbol{0}. \tag{7.11}$$

Additionally, if the nature of the intrinsic angular momentum density $\boldsymbol{a}$ is such that (see §8 for the appropriate conditions)

$$(\rho \boldsymbol{a})^s = \boldsymbol{0}, \tag{7.12}$$

then (7.11) reduces to the form

$$\nabla_s \cdot (\boldsymbol{I}_s \cdot \boldsymbol{C}^s) + \boldsymbol{P}^s_\times + \boldsymbol{G}^s = \boldsymbol{n} \cdot [\![(\bar{\boldsymbol{v}} - \boldsymbol{u}) \bar{\rho} \bar{\boldsymbol{a}} - \bar{\boldsymbol{C}}]\!]. \tag{7.13}$$

In order to apply this conservation equation to a specific dynamical system, constitutive equations for the microscale densities $\boldsymbol{G}$ and $\boldsymbol{C}$ are needed; these ultimately enable a rational derivation of the quantities $\boldsymbol{G}^s$ and $\boldsymbol{C}^s$ (as well as $\bar{\boldsymbol{C}}$).

In the absence of microscale external body couples ($\boldsymbol{G} = \boldsymbol{0}$), and in circumstances for which both the microscale internal angular momentum density vector $\boldsymbol{a}$ and the couple stress tensor $\boldsymbol{C}$ are constants (including, of course, being identically zero) with respect to position and time, it follows from (4.18) and (4.36) that $\boldsymbol{G}^s = \boldsymbol{C}^s = \boldsymbol{0}$, and $[\![\bar{\boldsymbol{C}}]\!] = [\![\bar{\boldsymbol{a}}]\!] = \boldsymbol{0}$ from (3.11). Substitution of these results, together with (7.4), into (7.13) yields

$$\boldsymbol{P}^s_\times = \boldsymbol{0}. \tag{7.14}$$

The leads via the identity $\boldsymbol{P}^{\mathrm{s}} - (\boldsymbol{P}^{\mathrm{s}})^{\dagger} = \boldsymbol{\varepsilon} \cdot \boldsymbol{P}_{\times}^{\mathrm{s}}$ to the conclusion that the surface-excess pressure tensor must be symmetric; explicitly,

$$\boldsymbol{P}^{\mathrm{s}} = (\boldsymbol{P}^{\mathrm{s}})^{\dagger}. \tag{7.15}$$

(d) *Conservation of species*

The interfacial conservation equation (5.26) for the species mass density (corresponding to the choice $\boldsymbol{\psi} \equiv \rho_i$) can be written in the form

$$\frac{\delta_{\mathrm{s}} \rho_i^{\mathrm{s}}}{\delta t} - \boldsymbol{u} \cdot \nabla_{\mathrm{s}} \rho_i^{\mathrm{s}} - 2H\boldsymbol{n} \cdot \boldsymbol{u} \rho_i^{\mathrm{s}} + \nabla_{\mathrm{s}} \cdot (\boldsymbol{I}_{\mathrm{s}} \cdot \boldsymbol{v} \rho_i)^{\mathrm{s}}$$

$$+ \nabla_{\mathrm{s}} \cdot (\boldsymbol{I}_{\mathrm{s}} \cdot \boldsymbol{j}_i^{\mathrm{s}}) - R_i^{\mathrm{s}} + \boldsymbol{n} \cdot [\![(\bar{\boldsymbol{v}} - \boldsymbol{u}) \bar{\rho}_i + \bar{\boldsymbol{j}}_i]\!] = 0. \tag{7.16}$$

If (6.15) holds, this equation becomes

$$\frac{\delta_{\mathrm{s}} \rho_i^{\mathrm{s}}}{\delta t} + (\boldsymbol{v} - \boldsymbol{u}) \cdot \nabla_{\mathrm{s}} \rho_i^{\mathrm{s}} + \{ \nabla_{\mathrm{s}} \cdot [\boldsymbol{v}_{\mathrm{s}}(\boldsymbol{x}_{\mathrm{s}}, 0) + \boldsymbol{n}\boldsymbol{n} \cdot \boldsymbol{u}] \} \rho_i^{\mathrm{s}}$$

$$+ \nabla_{\mathrm{s}} \cdot (\boldsymbol{I}_{\mathrm{s}} \cdot \boldsymbol{j}_i^{\mathrm{s}}) - R_i^{\mathrm{s}} + \boldsymbol{n} \cdot [\![(\bar{\boldsymbol{v}} - \boldsymbol{u}) \bar{\rho}_i + \bar{\boldsymbol{j}}_i]\!] = 0. \tag{7.17}$$

Surface-active substances, which tend to accumulate in the interfacial transition region, will possess relatively large microscale concentrations within this region; as such, the surface-excess density ρ_i^{s} of such species will be non-zero in the interfacial boundary condition (7.17). Conversely (in macroscale parlance), substances which tend not to be adsorbed at the interface will possess negligible values of ρ_i^{s}, and will thus be governed by the expression

$$\nabla_{\mathrm{s}} \cdot (\boldsymbol{I}_{\mathrm{s}} \cdot \boldsymbol{j}_i^{\mathrm{s}}) - R_i^{\mathrm{s}} + \boldsymbol{n} \cdot [\![(\bar{\boldsymbol{v}} - \boldsymbol{u}) \bar{\rho}_i + \bar{\boldsymbol{j}}_i]\!] = 0. \tag{7.18}$$

To apply any of the preceding equations of this subsection to a specific physical system, constitutive equations for the microscale densities R_i and $\boldsymbol{j}_i$ are needed, eventually enabling a rational derivation of the macroscale quantities $R_i^{\mathrm{s}}, \boldsymbol{j}_i^{\mathrm{s}}$, and $\bar{\boldsymbol{j}}_i$ appearing therein.

8. Discussion

(a) *Surface-excess quantities*

Since the operational expressions (4.18) and (4.36) for computing the surface-excess fields $\boldsymbol{\lambda}^{\mathrm{s}}$ and $\boldsymbol{\varphi}^{\mathrm{s}}$ from the microscale values are multiplied by the small parameter ϵ, non-negligible values of $\boldsymbol{\lambda}^{\mathrm{s}}$ and $\boldsymbol{\varphi}^{\mathrm{s}}$ will arise only when $|\tilde{\boldsymbol{\lambda}}_{\max}|/|\bar{\boldsymbol{\lambda}}| \gg 1$ and $|\tilde{\boldsymbol{\varphi}}_{\max}|/|\bar{\boldsymbol{\varphi}}| \gg 1$ respectively. For example, consider the pair of postulated field behaviours depicted in figure 5. If the form of the microscale density field $\boldsymbol{\lambda}$ is such that the latter does not attain a large maximum value within the interfacial transition region (as illustrated by curve A then the derived surface-excess field will be of $O(\epsilon)$, whence it may be concluded that $\boldsymbol{\lambda}_{\mathrm{A}}^{\mathrm{s}} = \boldsymbol{0}$ for all practical purposes. Physical examples of fields typified by curve A, and hence possessing vanishing surface-excess densities, are the total mass density ρ and the mass density ρ_i of conventional, surface-inactive, solutes. On the other hand, if $\boldsymbol{\lambda}$ does attain a large maximum value within the interfacial region, as illustrated by curve B, the surface-excess field will be sensible; i.e. $\boldsymbol{\lambda}_{\mathrm{B}}^{\mathrm{s}} \neq \boldsymbol{0}$. One example of such a field is the mass density ρ_i of a surface-active species i; thus, $\rho_i^{\mathrm{s}} > 0$ for surface-active solutes.

Large magnitudes of the microscale continuum field variables $\boldsymbol{\lambda}$ and/or $\boldsymbol{\varphi}$ generally arise in dynamical and energetic transport processes only when surface-active
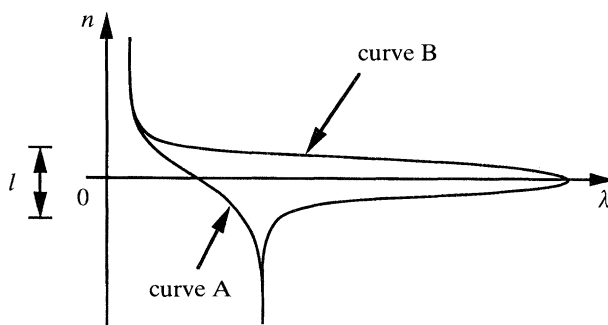
Figure 5. Schematic showing the two main types of behaviour for a microscale field $\lambda \equiv \lambda(x_s, n)$ within the diffuse interfacial region. Curve A depicts a field with no large maximum value, whereas curve B depicts a field which attains a relatively large maximum value within the transition region. In this figure x_s is constant.

substances are adsorbed at the interface. Thus, for momentum transport at 'clean' interfaces, equilibrium or thermodynamic interfacial tension appears to be the only important surface-excess quantity. (Interfacial tension constitutes a surface-excess thermodynamic pressure in Part II (cf. (4.36) with $\varphi \equiv p$).) However, sensible interfacial shear and dilatational viscosity coefficients (characterizing the macroscale rheological properties of 'newtonian' interfaces (Scriven 1960)) are observed when surfactants are present at the interface (Wasan *et al.* 1971; Wei & Slattery 1976).

(b) *Placement of the dividing surface*

According to traditional interfacial transport theories (Eliassen 1963; Murphy 1966; Slattery 1967; Deemer & Slattery 1978; Alts & Hutter 1988), which aim at an 'exact' description of interfacial (and, concomitantly, bulk) transport phenomena, the location of the Gibbs (1957) 'dividing surface' must be precisely defined in order to provide exact definitions of requisite surface-excess properties. However, in the asymptotic theory presented here, the precise location of the 'dividing' *parent* surface proves both unnecessary and irrelevant. Rather, the only constraint placed upon the location of the coordinate parent surface – the latter representing the position assigned to the macroscale interface in the limit $\epsilon \to 0$ – is that it must be located somewhere within the inner interfacial transition region; additionally, the principal curvatures κ_1 and κ_2 of the parent surface must be macroscale quantities (cf. (2.1)).

As proof that the precise location of the parent surface is inconsequential in the unambiguous definition of surface-excess properties, consider the consequences of a shift by an amount $|\Delta\tilde{n}| = O(1)$ in the location of the choice of parent surface in physical space. Changing the position of the parent surface from $\tilde{n}_0 = 0$ to $\tilde{n}_0 = a$, where both values of $\tilde{n}_0$ lie within the inner region (i.e. $a = O(1)$), will result in a change,

$$\Delta\lambda^s = \epsilon L \left\{ \int_{\tilde{n}=0}^{a} [\bar{\lambda}_1(0) - \bar{\lambda}_2(0)] \, d\tilde{n} + \int_{\tilde{n}=a}^{+\infty} [\bar{\lambda}_1(0) - \bar{\lambda}_1(a)] \, d\tilde{n} + \int_{\tilde{n}=-\infty}^{a} [\bar{\lambda}_2(0) - \bar{\lambda}_2(a)] \, d\tilde{n} \right\},$$
$$(8.1)$$

in the value of the surface-excess quantity λ^s. Order-of-magnitude values for the various integrands appearing above are, respectively,

$$\bar{\lambda}_1(0) - \bar{\lambda}_2(0) = O(1) \qquad (8.2)$$

and
$$\bar{\lambda}_\alpha(0) - \bar{\lambda}_\alpha(a) = O(\epsilon) \quad (\alpha = 1, 2). \tag{8.3}$$

Thus, upon using table 1, the difference $\Delta\lambda^s$ derived from (8.1), namely

$$\Delta\lambda^s = O(1)\,O(\epsilon) + O(\epsilon)\,O(\epsilon^r) + O(\epsilon)\,O(\epsilon^r) \equiv O(\epsilon), \tag{8.4}$$

becomes negligible as $\epsilon \to 0$. Accordingly, varying the position of the parent surface within the interfacial transition region will have no sensible effect upon the numerical value of the $O(1)$ surface-excess quantity λ^s, at least to the order of approximation of our theory. Similar remarks apply to the insensitivity of φ^s to the exact placement of the dividing surface within the interfacial transition region.

Although most prior theories (Kirkwood & Buff 1949; Eliassen 1963; Murphy 1966) attempt to precisely define the requisite position of the dividing surface, so as to render these theories 'exact', such a definition is not necessarily possible. In particular, Schofield & Henderson (1982) conclude that, from a statistical mechanical point of view, the position of the 'surface of tension' (Kirkwood & Buff 1949) is ill-defined, and hence '...could be placed anywhere in the interface region by choosing different contours in the definition of the [microscale] pressure tensor'.

(c) Curvature constraints

Our asymptotic view stands in marked contrast to the more traditional view of other authors (Eliassen 1963; Murphy 1966; Slattery 1967; Deemer & Slattery 1978; Alts & Hutter 1988), which claim to be exact theories, and hence valid for all curvatures. However, in our asymptotic view, the conventional view of an interface as a singular two-dimensional surface can only be justified for circumstances in which the principal curvatures of the (macroscale) interface are of macroscopic order, i.e. characterized by the same linear dimension L as the bulk-fluid depths. Indeed, the traditional theories suppose that a homogeneous bulk-fluid phase exists on either side of the interfacial transition region, thus (implicitly, if not explicitly) imposing restrictions upon the magnitude of the curvature for which their theories are applicable.

(d) Surface-fixed coordinate system

In this paper, a surface-fixed coordinate system is developed which moves and deforms together with the two-dimensional parent surface (assumed to physically coincide with the macroscale interface) to which it is affixed. Since the parent surface is not defined to be a 'material' surface, our theory remains valid for systems in which convective mass transport (for which $\boldsymbol{n}\cdot(\boldsymbol{v}-\boldsymbol{u}) \neq O(\epsilon)$) occurs across the macroscale interface. This applicability to interfacial mass-transfer phenomena contrasts with the theories of Eliassen (1963) and Goodrich (1981), which are limited to material interfaces with a *fixed* mode of motion, involving the motion of parallel surfaces bounded by an envelope of orthogonal *straight* lines. In addition, our use of a surface-fixed control volume bounded by non-material boundaries eliminates the need for the approximations introduced by Slattery (1967) and Deemer & Slattery (1978) when projecting the contents of a material element onto their dividing surface. Close to our view, both Slattery (1967) and Deemer & Slattery (1978) use a non-material dividing surface to account for situations involving convective mass transport across the interface. However, since they use a *material* body as their control volume, the latter will not necessarily coincide with the region being projected onto the dividing surface (compare the two regions $R^{(I)}$ and $R^{(I)*}$ given in

Table 5. *Definitions of geometric quantities for two- and three-dimensional spaces*

quantity	three-dimensional form	two-dimensional form
tensor indices	$i = 1, 2, 3$	$\alpha = 1, 2$
differential lineal element	$d\boldsymbol{x} = \boldsymbol{g}_i \, dq^i$	$d\boldsymbol{x}_s = \boldsymbol{a}_\alpha \, dq^\alpha$
basis vectors	$\boldsymbol{g}_i = \partial \boldsymbol{x} / \partial q^i$	$\boldsymbol{a}_\alpha = \partial \boldsymbol{x}_s / \partial q^\alpha$
metric tensor	$g_{ij} = \boldsymbol{g}_i \cdot \boldsymbol{g}_j$	$a_{\alpha\beta} = \boldsymbol{a}_\alpha \cdot \boldsymbol{a}_\beta$
determinant	$g = \det(g_{ij}) = |\boldsymbol{g}_1 \cdot \boldsymbol{g}_2 \times \boldsymbol{g}_3|^2$	$a = \det(a_{\alpha\beta}) = |\boldsymbol{a}_1 \times \boldsymbol{a}_2|^2$
reciprocal basis vectors	$(\boldsymbol{g}^1, \boldsymbol{g}^2, \boldsymbol{g}^3)$, with $\boldsymbol{g}^i \cdot \boldsymbol{g}_j = \delta_j^i$	$(\boldsymbol{a}^1, \boldsymbol{a}^2)$, with $\boldsymbol{a}^\alpha \cdot \boldsymbol{a}_\beta = \delta_\beta^\alpha$
idemfactor	$\boldsymbol{I} = \boldsymbol{g}_i \boldsymbol{g}^i = \boldsymbol{g}^i \boldsymbol{g}_i \equiv \nabla \boldsymbol{x}$	$\boldsymbol{I}_s = \boldsymbol{I} - \boldsymbol{n}\boldsymbol{n} \equiv$ $\boldsymbol{a}_\alpha \boldsymbol{a}^\alpha = \boldsymbol{a}^\alpha \boldsymbol{a}_\alpha \equiv \nabla_s \boldsymbol{x}_s$
gradient operator	$\nabla = \boldsymbol{g}^i \, \partial / \partial q^i$	$\nabla_s = \boldsymbol{I}_s \cdot \nabla \equiv \boldsymbol{a}^\alpha \partial / \partial q^\alpha$
alternator	$\boldsymbol{\varepsilon} = \boldsymbol{g}^i \boldsymbol{g}^j \boldsymbol{g}^k \, e_{ijk}$	$\boldsymbol{\varepsilon}_s = \boldsymbol{\varepsilon} \cdot \boldsymbol{n} = \boldsymbol{a}^\alpha \boldsymbol{a}^\beta \, e_{\alpha\beta}$
alternating tensor	$e_{ijk} = \boldsymbol{g}_i \cdot \boldsymbol{g}_j \times \boldsymbol{g}_k \equiv \sqrt{(g)} \, e_{ijk}$	$e_{\alpha\beta} = \boldsymbol{a}_\alpha \times \boldsymbol{a}_\beta \cdot \boldsymbol{n} \equiv \sqrt{(a)} \, e_{\alpha\beta}$

Deemer & Slattery (1978)); this leads to unnecessary approximations (see their equations [27]–[29]). Similar approximations arise when a space-fixed control volume (Dumais 1980) is employed. Our parametrization of space via a surface-fixed coordinate system thus appears more versatile than the methods cited above.

Appendix A. Geometric relations

This appendix provides a convenient compendium of important relations used in this paper pertaining to our surface-fixed coordinate system (figure 2). Table 5 defines the necessary geometric quantities for two- and three-dimensional spaces. Throughout this and Appendix B, the summation convention on repeated indices will apply, except where explicitly disclaimed.

In addition to the quantities defined in table 5, the vector

$$\boldsymbol{n} = \boldsymbol{a}_1 \times \boldsymbol{a}_2 / \sqrt{a} \quad (a = |\boldsymbol{a}_1 \times \boldsymbol{a}_2|^2) \tag{A 1}$$

constitutes the unit normal to the parent coordinate surface; moreover,

$$\delta_j^i = \begin{cases} 1 & (i = j), \\ 0 & (i \neq j), \end{cases} \tag{A 2}$$

is the Kronecker delta. The permutation symbol

$$e_{\alpha\beta} = \begin{cases} 0 & (\alpha = \beta), \\ 1 & (\alpha = 1, \beta = 2), \\ -1 & (\alpha = 2, \beta = 1) \end{cases} \tag{A 3}$$

and

$$e_{ijk} = \begin{cases} 0 & \text{if any two indices are equal,} \\ 1 & \text{if } (i, j, k) \text{ is an even permutation of } (1, 2, 3), \\ -1 & \text{if } (i, j, k) \text{ is an odd permutation of } (1, 2, 3) \end{cases} \tag{A 4}$$

are, respectively, the second- and third-order permutation symbols. The alternator is related to the cross-product operation by the expression

$$\varepsilon : uv = -u \times v, \tag{A 5}$$

where u and v are arbitrary vectors.

In developing our surface-fixed coordinate system, the q^3-coordinate curve has been defined (see §2) such as to be orthogonal to all q^3-coordinate surfaces (the latter characterized by the assignation $q^3 = $ constant). Thus, understanding of the metrical properties of the interfacial system can be enhanced by introducing the notation for the three-dimensional coordinate parametrization given below.

Let the basis vectors g_i for three-dimensional physical space, as parametrized by the surface-fixed coordinates q^i, be written in the form

$$*a_\alpha \equiv g_\alpha = \partial x / \partial q^\alpha \quad (\alpha = 1, 2), \qquad *n_3 \equiv g_3 = \partial x / \partial q^3. \tag{A 6a, b}$$

In this notation, the basis vectors for any q^3-coordinate surface are represented by $*a_\alpha$ and the (non-normalized) tangent vector to any q^3-coordinate curve by $*n_3$. Since the q^3-coordinate surfaces are orthogonal to the q^3-coordinate curves, it follows that

$$*a_\alpha \cdot *n_3 = 0 \tag{A 7}$$

at every point x. The metric tensor g_{ij} then becomes

$$g_{\alpha\beta} = *a_\alpha \cdot *a_\beta \equiv *a_{\alpha\beta}, \quad g_{33} = *n_3 \cdot *n_3 \equiv (*h_3)^2, \quad g_{\alpha 3} = g_{3\alpha} = 0, \tag{A 8a–c}$$

with $*h_3$ reckoned to be positive. With use of the above relations,

$$g = \det (g_{ij}) = *a(*h_3)^2, \tag{A 9}$$

wherein

$$*a = \det (*a_{\alpha\beta}) \equiv |*a_1 \times *a_2|^2. \tag{A 10}$$

Orthogonal to the q^3-coordinate surface is the *unit* normal vector

$$*n = *n_3 / *h_3 \equiv *a_1 \times *a_2 / \sqrt{*a}, \tag{A 11}$$

in which the basis vector triad is taken to be right-handed in the order $(*a_1, *a_2, *n_3)$.

Analogous notation holds for reciprocal basis vectors and tensors. Explicit representations for the reciprocal basis vectors are

$$*a^1 = (*a_{22} *a_1 - *a_{21} *a_2) / *a, \tag{A 12}$$

$$*a^2 = (*a_{11} *a_2 - *a_{12} *a_1) / *a, \tag{A 13}$$

$$*n^3 = *n_3 / g_{33}. \tag{A 14}$$

In this notation, the q^3-coordinate surface idemfactor may be written as

$$*I_s = I - *n*n = *a_\alpha *a^\alpha = *a^\alpha *a_\alpha, \tag{A 15}$$

and the q^3-coordinate surface alternator as

$$*\varepsilon_s = \varepsilon \cdot *n = *a_\alpha *a_\beta *e^{\alpha\beta}. \tag{A 16}$$

The q^3-coordinate surface analogue of (A 5) is given by the expression

$$*\varepsilon_s : *u*v = -(*u \times *v) \cdot *n. \tag{A 17}$$

Analogous to the operator ∇_s defined in table 5 is the q^3-coordinate surface gradient operator,

$$*\nabla_s \stackrel{\text{def}}{=} *I_s \cdot \nabla \equiv *a^\alpha \frac{\partial}{\partial q^\alpha}. \tag{A 18}$$

(a) Differential elements

Differential physical-space elements can be constructed by combining in different manners the differential position vectors

$$d\boldsymbol{x}_{(1)} = {}^*\boldsymbol{a}_\alpha \, dq^\alpha_{(1)}, \tag{A 19}$$

$$d\boldsymbol{x}_{(2)} = {}^*\boldsymbol{a}_\alpha \, dq^\alpha_{(2)}, \tag{A 20}$$

$$d\boldsymbol{x}_{(3)} = {}^*\boldsymbol{n}_3 \, dq^3. \tag{A 21}$$

Here, $d\boldsymbol{x}_{(1)}$ and $d\boldsymbol{x}_{(2)}$ are arbitrary differential lineal displacements lying upon (strictly, tangent to) the q^3-coordinate surface, whereas $d\boldsymbol{x}_{(3)}$ is a displacement along the q^3-coordinate curve.

For the above relations,

$$dn = {}^*\boldsymbol{n} \cdot d\boldsymbol{x}_{(3)} = {}^*h_3 \, dq^3 \tag{A 22}$$

is a differential line element along a q^3-coordinate curve, and

$$d{}^*A = {}^*\boldsymbol{n} \cdot [d\boldsymbol{x}_{(1)} \times d\boldsymbol{x}_{(2)}] = {}^*\boldsymbol{n} \cdot [{}^*\boldsymbol{a}_\alpha \times {}^*\boldsymbol{a}_\beta] \, dq^\alpha_{(1)} \, dq^\beta_{(2)}$$
$$= {}^*\epsilon_{\alpha\beta} \, dq^\alpha_{(1)} \, dq^\beta_{(2)} = \sqrt{({}^*a)} \, e_{\alpha\beta} \, dq^\alpha_{(1)} \, dq^\beta_{(2)} \tag{A 23}$$

is a differential surface element $d{}^*A$ lying upon a q^3-coordinate surface. A differential volume element dV which is bounded laterally by a q^3-coordinate curve envelope and by q^3-coordinate surfaces on its top and bottom is given by the expression

$$dV = [d\boldsymbol{x}_{(1)} \times d\boldsymbol{x}_{(2)}] \cdot d\boldsymbol{x}_{(3)} = {}^*\epsilon_{\alpha\beta} \, {}^*h_3 \, dq^\alpha_{(1)} \, dq^\beta_{(2)} \, dq^3 = d{}^*A \, dn. \tag{A 24}$$

Consider a surface composed of an envelope of q^3-coordinate curves (such as the open surface constituting the lateral boundaries of the control volume depicted in figure 4). The closed curve ${}^*C(s)$ will be chosen such as to represent the intersection of this surface with an arbitrary q^3-coordinate surface, in which s parametrizes the position of a point along the curve. The differential position vector in the (positive) direction of the curve ${}^*C$ may be written as

$$d\boldsymbol{x}_{(c)} = {}^*\boldsymbol{t}_{(c)} \, ds, \tag{A 25}$$

wherein

$${}^*\boldsymbol{t}_{(c)} = \partial\boldsymbol{x}/\partial s = {}^*h_c \, {}^*\boldsymbol{t}, \tag{A 26}$$

with ${}^*h_c(s, q^3)$ the metrical coefficient at a point of the curve, and ${}^*\boldsymbol{t}$ the unit tangent vector to the curve in a positive sense.

A differential element of length $d{}^*C$ along the curve will thus be given by the expression

$$d{}^*C = {}^*\boldsymbol{t} \cdot d\boldsymbol{x}_{(c)} = {}^*h_c \, ds. \tag{A 27}$$

The directed differential areal element $d\boldsymbol{S}$ of this surface possesses the representation

$$d\boldsymbol{S} = d\boldsymbol{x}_{(c)} \times d\boldsymbol{x}_{(3)} = ({}^*\boldsymbol{t} \times {}^*\boldsymbol{n}) \, {}^*h_c \, {}^*h_3 \, ds \, dq^3 = {}^*\boldsymbol{m} \, d{}^*C \, dn, \tag{A 28}$$

in which

$${}^*\boldsymbol{m} = {}^*\boldsymbol{t} \times {}^*\boldsymbol{n} \tag{A 29}$$

is the outwardly-directed unit normal vector to the differential surface element. Since ${}^*\boldsymbol{m}$ is orthogonal to both ${}^*\boldsymbol{n}$ and ${}^*\boldsymbol{t}$, it is also the vector normal to the differential element $d{}^*C$, and lies in the tangent plane to the q^3-coordinate surface.

Appendix B. Projections onto the parent surface

To derive the macroscale interfacial conservation equations, we require the projections of arbitrary areal and lineal elements lying upon a q^3-coordinate surface onto the coordinate parent surface along an 'envelope' determined by the q^3-coordinate curves (figure 3).

(a) Surface element

In the sense of the preceding paragraph, the projection of the differential areal element (cf. (A 23))

$$\mathrm{d}*A = \sqrt{(*a)}\, e_{\alpha\beta}\, \mathrm{d}q^{\alpha}_{(1)}\, \mathrm{d}q^{\beta}_{(2)}, \tag{B 1}$$

lying on an arbitrary q^3-coordinate surface, onto the parent surface $q^3 = q^3_0$ is given by the expression

$$\mathrm{d}*A = *M\, \mathrm{d}A, \tag{B 2}$$

in which

$$\mathrm{d}A = \sqrt{(a)}\, e_{\alpha\beta}\, \mathrm{d}q^{\alpha}_{(1)}\, \mathrm{d}q^{\beta}_{(2)}, \tag{B 3}$$

and

$$*M = \sqrt{(*a/a)}. \tag{B 4}$$

Equation (B 4) permits explicit calculation of the areal 'magnification factor' $*M$ given below (cf. (B 22)).

According to (A 10), $*a$ is defined by the relation

$$*a = |*\boldsymbol{a}_1 \times *\boldsymbol{a}_2|^2 = (*\boldsymbol{a}_1 \cdot *\boldsymbol{a}_1)(*\boldsymbol{a}_2 \cdot *\boldsymbol{a}_2) - (*\boldsymbol{a}_1 \cdot *\boldsymbol{a}_2)^2. \tag{B 5}$$

Differentiation of $\sqrt{*a}$ with respect to an arbitrary variable ξ gives

$$\frac{\partial \sqrt{*a}}{\partial \xi} = \frac{1}{2\sqrt{*a}}\left(\frac{\partial *a}{\partial \xi}\right). \tag{B 6}$$

From (B 5),

$$\left(\frac{1}{2}\right)\frac{\partial *a}{\partial \xi} = *a_{22}\left(*\boldsymbol{a}_1 \cdot \frac{\partial *\boldsymbol{a}_1}{\partial \xi}\right) + *a_{11}\left(*\boldsymbol{a}_2 \cdot \frac{\partial *\boldsymbol{a}_2}{\partial \xi}\right) - *a_{12}\left(*\boldsymbol{a}_1 \cdot \frac{\partial *\boldsymbol{a}_2}{\partial \xi} + *\boldsymbol{a}_2 \cdot \frac{\partial *\boldsymbol{a}_1}{\partial \xi}\right)$$

$$= (*a_{22}\,*\boldsymbol{a}_1 - *a_{12}\,*\boldsymbol{a}_2) \cdot \frac{\partial *\boldsymbol{a}_1}{\partial \xi} + (*a_{11}\,*\boldsymbol{a}_2 - *a_{21}\,*\boldsymbol{a}_1) \cdot \frac{\partial *\boldsymbol{a}_2}{\partial \xi}. \tag{B 7}$$

Upon using (A 12) and (A 13), the above relation may be expressed as

$$\left(\frac{1}{2}\right)\frac{\partial *a}{\partial \xi} = *a\left(*\boldsymbol{a}^{\alpha} \cdot \frac{\partial *\boldsymbol{a}_{\alpha}}{\partial \xi}\right), \tag{B 8}$$

whence (B 6) becomes

$$\frac{\partial \sqrt{*a}}{\partial \xi} = \sqrt{*a}\left(*\boldsymbol{a}^{\alpha} \cdot \frac{\partial *\boldsymbol{a}_{\alpha}}{\partial \xi}\right). \tag{B 9}$$

In our particular case, ξ will be chosen as q^3.

Use of the definitions (A 6) produces the expression

$$\frac{\partial *\boldsymbol{a}_{\alpha}}{\partial q^3} = \frac{\partial}{\partial q^3}\left(\frac{\partial \boldsymbol{x}}{\partial q^{\alpha}}\right) = \frac{\partial}{\partial q^{\alpha}}\left(\frac{\partial \boldsymbol{x}}{\partial q^3}\right) = \frac{\partial *\boldsymbol{n}_3}{\partial q^{\alpha}}. \tag{B 10}$$

Application of (A 11) yields

$$\frac{\partial *\boldsymbol{n}_3}{\partial q^{\alpha}} = \frac{\partial(*h_3\,*\boldsymbol{n})}{\partial q^{\alpha}} = \left(\frac{\partial *h_3}{\partial q^{\alpha}}\right)*\boldsymbol{n} + *h_3\left(\frac{\partial *\boldsymbol{n}}{\partial q^{\alpha}}\right). \tag{B 11}$$

Upon using (A 18) together with the known symmetry of the curvature dyadic $\boldsymbol{b}$ (cf. (2.9)), we obtain

$$\partial {}^*\boldsymbol{n}/\partial q^\alpha = {}^*\boldsymbol{a}_\alpha \cdot ({}^*\nabla_{\mathrm{s}}\,{}^*\boldsymbol{n}) = ({}^*\nabla_{\mathrm{s}}\,{}^*\boldsymbol{n}) \cdot {}^*\boldsymbol{a}_\alpha. \tag{B 12}$$

Differentiation of the normalization relation ${}^*\boldsymbol{n} \cdot {}^*\boldsymbol{n} = 1$ with respect to q^i gives

$${}^*\boldsymbol{n} \cdot (\partial {}^*\boldsymbol{n}/\partial q^i) = 0. \tag{B 13}$$

Substitute (B 11) into (B 10), form the scalar product of the resulting expression with ${}^*\boldsymbol{n}$, and use (B 13) (with $i = \alpha$) to simplify the result. This yields

$$(\partial {}^*h_3/\partial q^\alpha) = {}^*\boldsymbol{n} \cdot (\partial {}^*\boldsymbol{a}_\alpha/\partial q^3). \tag{B 14}$$

The orthogonalization condition ${}^*\boldsymbol{a}_\alpha \cdot {}^*\boldsymbol{n} = 0$ may be differentiated with respect to q^3 to give

$${}^*\boldsymbol{n} \cdot \left(\frac{\partial {}^*\boldsymbol{a}_\alpha}{\partial q^3}\right) = -{}^*\boldsymbol{a}_\alpha \cdot \left(\frac{\partial {}^*\boldsymbol{n}}{\partial q^3}\right). \tag{B 15}$$

From the above relations, we thereby obtain

$$\left(\frac{\partial {}^*h_3}{\partial q^\alpha}\right) = -{}^*\boldsymbol{a}_\alpha \cdot \left(\frac{\partial {}^*\boldsymbol{n}}{\partial q^3}\right), \tag{B 16}$$

whence

$${}^*\boldsymbol{n}\left(\frac{\partial \ln {}^*h_3}{\partial q^\alpha}\right) = -({}^*\nabla_n\,{}^*\boldsymbol{n}) \cdot {}^*\boldsymbol{a}_\alpha, \tag{B 17}$$

wherein

$${}^*\nabla_n = {}^*\boldsymbol{n}\,{}^*\boldsymbol{n} \cdot \nabla. \tag{B 18}$$

Substitute (B 12) and (B 17) into (B 11) and introduce the resulting expression into (B 10) to obtain

$$\partial {}^*\boldsymbol{a}_\alpha/\partial q^3 = ({}^*\nabla_{\mathrm{s}}\,{}^*\boldsymbol{n} - {}^*\nabla_n\,{}^*\boldsymbol{n}) \cdot {}^*\boldsymbol{a}_\alpha\,{}^*h_3. \tag{B 19}$$

Scalarly multiply the above equation with ${}^*\boldsymbol{a}^\alpha$, and recall that ${}^*\boldsymbol{a}^\alpha \cdot {}^*\boldsymbol{n} = 0$. This yields

$${}^*\boldsymbol{a}^\alpha \cdot \frac{\partial {}^*\boldsymbol{a}_\alpha}{\partial q^3} = ({}^*\nabla_{\mathrm{s}}\,{}^*\boldsymbol{n}) : {}^*\boldsymbol{a}_\alpha\,{}^*\boldsymbol{a}^\alpha\,{}^*h_3 = ({}^*\nabla_{\mathrm{s}} \cdot {}^*\boldsymbol{n})\,{}^*h_3. \tag{B 20}$$

Use the definition for the mean curvature ${}^*H$ given in (2.11) and subsequently substitute the resulting expression into (B 9) to derive the equation

$$\partial \sqrt{{}^*a}/\partial q^3 = -2{}^*H\sqrt{({}^*a)}\,{}^*h_3. \tag{B 21}$$

The latter can be integrated along a q^3-coordinate curve from the parent surface ($q^3 = q_0^3$) to an arbitrary q^3-coordinate surface, thereby producing the relation

$${}^*M = \sqrt{({}^*a/a)} = \exp\left(-\int_{q_0^3}^{q^3} 2{}^*H\,{}^*h_3\,\mathrm{d}q^3\right). \tag{B 22}$$

(b) Line element

Similarly to the above, the projection of a differential lineal element (cf. (A 27)),

$$\mathrm{d}{}^*C = {}^*h_c\,\mathrm{d}s, \tag{B 23}$$

lying on the q^3-coordinate surface, onto the parent surface along curvilinear lines determined by the q^3-coordinate curves is given by the expression

$$\mathrm{d}{}^*C = {}^*N\,\mathrm{d}C, \tag{B 24}$$

wherein
$$dC = h_c\, ds, \tag{B 25}$$
and
$$*N = *h_c/h_c. \tag{B 26}$$

An explicit expression for the lineal magnification factor $*N$ may be established by considering the derivative

$$\frac{\partial *h_c}{\partial q^3} = \frac{1}{2*h_c}\left[\frac{\partial(*h_c)^2}{\partial q^3}\right]. \tag{B 27}$$

From (A 26), one can write

$$\left(\frac{1}{2}\right)\frac{\partial(*h_c)^2}{\partial q^3} = *t_{(c)} \cdot \frac{\partial *t_{(c)}}{\partial q^3}. \tag{B 28}$$

Use of (A 6), (A 11) and (A 26) yields

$$\frac{\partial *t_{(c)}}{\partial q^3} = \frac{\partial}{\partial q^3}\left(\frac{\partial x}{\partial s}\right) = \frac{\partial}{\partial s}\left(\frac{\partial x}{\partial q^3}\right) = \frac{\partial(*h_3 *n)}{\partial s}. \tag{B 29}$$

Upon using the expression

$$\partial(*h_3 *n)/\partial s = *t_{(c)} \cdot \nabla(*h_3 *n) = *t_{(c)} \cdot (\nabla *n)\,*h_3 + *t_{(c)} \cdot (\nabla *h_3)\,*n, \tag{B 30}$$

together with (A 26), (B 28) and (B 29), and subsequently noting that $*t \cdot *n = 0$ (since $*t$ is a vector tangent to the q^3-coordinate surface), the derivative (B 27) becomes

$$\partial *h_c/\partial q^3 = *t*t:(\nabla *n)\,*h_3\,*h_c = -*\kappa_{(n)}(*t)\,*h_3\,*h_c, \tag{B 31}$$

wherein

$$*\kappa_{(n)}(*t) = -*t*t:(*\nabla_s\,*n) = *t*t:*b \tag{B 32}$$

is the curvature at a point of the q^3-coordinate curve. Integration of (B 31) along a q^3-coordinate curve from the parent surface to an arbitrary q^3-coordinate surface yields

$$*N = *h_c/h_c = \exp\left(-\int_{q_0^3}^{q^3} *\kappa_{(n)}(*t)\,*h_3\, dq^3\right). \tag{B 33}$$

The unit surface vector $*m$ (cf. (A 29)) that forms the outward normal to the curve $d*C$ will vary with q^3 according to the equation

$$\frac{\partial *m}{\partial q^3} = \frac{\partial *t}{\partial q^3} \times *n + *t \times \frac{\partial *n}{\partial q^3}. \tag{B 34}$$

Upon using (A 26) and (B 29)–(B 31), one obtains

$$\frac{\partial *t}{\partial q^3} = -\frac{1}{(*h_c)^2}\left(\frac{\partial *h_c}{\partial q^3}\right)*t_{(c)} + \frac{1}{*h_c}\left(\frac{\partial *t_{(c)}}{\partial q^3}\right)$$
$$= -*t*t:(\nabla *n)\,*h_3\,*t + *t \cdot (\nabla *n)\,*h_3 + *t \cdot (\nabla *h_3)\,*n, \tag{B 35}$$

and
$$\partial *n/\partial q^3 = *n_3 \cdot \nabla *n. \tag{B 36}$$

Use of (A 29) together with the vector identity

$$a \times (b \times c) = b(a \cdot c) - c(a \cdot b), \tag{B 37}$$

(in which a, b and c are arbitrary vectors) yields the relations

$$(*t \cdot \nabla *n) \times *n = *m(*t*t:\nabla *n) - *t(*m*t:\nabla *n) \tag{B 38}$$

and
$$*t \times (*n \cdot \nabla *n) = - *n(*m*n : \nabla *n). \tag{B 39}$$

In the above equation we have used the identity (cf. (B 13) with $i = 3$)

$$*n*n : \nabla *n = 0. \tag{B 40}$$

Substitute (B 35), (B 36) and (B 38)–(B 40) into (B 34) to obtain

$$\partial *m/\partial q^3 = -(*t*t + *n*n) \cdot (\nabla *n) \cdot *m*h_3. \tag{B 41}$$

Upon integrating the above equation along a q^3-coordinate curve, the expression

$$*m = m - \int_{q_0^3}^{q^3} (*t*t + *n*n) \cdot (\nabla *n) \cdot *m*h_3 \, dq^3 \tag{B 42}$$

is obtained.

References

Alts, T. & Hutter, K. 1988 Continuum description of the dynamics and thermodynamics of phase boundaries between ice and water, Part I. Surface balance laws and their interpretation in terms of three-dimensional balance laws averaged over the phase change boundary layer. *J. Non-equilibr. Therm.* **13**, 221–257.

Aris, R. 1962 *Vectors, tensors, and the basic equations of fluid mechanics.* Prentice-Hall.

Bird, R. B., Stewart, W. E. & Lightfoot, E. N. 1960 *Transport phenomena.* Wiley.

Brenner, H. 1979 A micromechanical derivation of the differential equations of interfacial statics. *J. Colloid Interface Sci.* **68**, 422–439.

Brenner, H. & Leal, L. G. 1977 A model of surface diffusion on solids. *J. Colloid Interface Sci.* **62**, 238–258.

Brenner, H. & Leal, L. G. 1978*a* A micromechanical derivation of Fick's law for interfacial diffusion of surfactant molecules. *J. Colloid Interface Sci.* **65**, 191–209.

Brenner, H. & Leal, L. G. 1978*b* Interfacial resistance to interphase mass transfer in quiescent two-phase systems. *A.I.Ch.E. Jl* **24**, 246–254.

Brenner, H. & Leal, L. G. 1982 Conservation and constitutive equations for adsorbed species undergoing surface diffusion and convection at a fluid-fluid interface. *J. Colloid Interface Sci.* **88**, 136–184.

Buff, F. P. 1956 Curved fluid interfaces. I. The generalized Gibbs–Kelvin equation. *J. chem. Phys.* **25**, 146–153.

Chapman, S. & Cowling, T. G. 1961 *The mathematical theory of non-uniform gases*, 2nd edn. Cambridge University Press.

Deemer, A. R. & Slattery, J. C. 1978 Balance equations and structural models for phase interfaces. *Int. J. Multiphase Flow* **4**, 171–192.

Dell'Isola, F. & Romano, A. 1987*a* On the derivation of thermomechanical balance equations for continuous systems with a nonmaterial interface. *Int. J. Engng Sci.* **25**, 1459–1468.

Dell'Isola, F. & Romano, A. 1987*b* A phenomenological approach to phase transition in classical field theory. *Int. J. Engng Sci.* **25**, 1469–1475.

Dumais, J.-F. 1980 Two and three-dimensional interfacial dynamics. *Physica* A **104**, 143–180.

Eliassen, J. D. 1963 Interfacial mechanics. Ph.D. dissertation, University of Minnesota, Minneapolis, Minnesota, U.S.A.

Ghez, R. 1966 A generalized Gibbsian surface. *Surf. Sci.* **4**, 125–140.

Gibbs, J. W. 1957 *The collected works of J. Willard Gibbs*, vol. I. Yale University Press.

Gibbs, J. W. & Wilson, E. B. 1960 *Vector analysis.* Dover.

Goodrich, F. C. 1981 The theory of capillary excess viscosities. *Proc. R. Soc. Lond.* A **374**, 341–370.

Gurtin, M. E. & Struthers, A. 1990 Multiphase thermomechanics with interfacial structure 3. Evolving phase boundaries in the presence of bulk deformation. *Arch. ration. Mech. Analysis* **112**, 97–160.

Happel, J. & Brenner, H. 1986 *Low Reynolds number hydrodynamics.* Nijhoff.

Kevorkian, J. & Cole, J. D. 1981 *Perturbation methods in applied mathematics*. Springer-Verlag.

Kirkwood, J. G. & Buff, F. P. 1949 The statistical mechanical theory of surface tension. *J. chem. Phys.* **17**, 338–343.

McConnell, A. J. 1957 *Applications of tensor analysis*. Dover.

Moeckel, G. P. 1975 Thermodynamics of an interface. *Arch. ration. Mech. Analysis* **57**, 255–280.

Murphy, C. L. 1966 Thermodynamics of low tension and highly curved interfaces. Ph.D. dissertation, University of Minnesota, Minneapolis, Minnesota, U.S.A.

Nayfeh, A. A. 1973 *Perturbation methods*. Wiley.

Ono, S. & Kondo, S. 1960 Molecular theory of surface tension in liquids. In *Encyclopedia of physics* (ed. S. Flügge), vol. 10, pp. 134–280. Springer.

Scriven, L. E. 1960 Dynamics of a fluid interface. Equation of motion for Newtonian surface fluids. *Chem. Engng Sci.* **12**, 98–108.

Schofield, P. & Henderson, J. R. 1982 Statistical mechanics of inhomogeneous fluids. *Proc. R. Soc. Lond.* A **379**, 231–246.

Slattery, J. C. 1964*a* Surfaces – I. Momentum and moment-of-momentum balances for moving surfaces. *Chem. Engng Sci.* **19**, 379–385.

Slattery, J. C. 1964*b* Surfaces – II. Kinematics of diffusion in a heterogeneous surface. *Chem. Engng Sci.* **19**, 453–455.

Slattery, J. C. 1967 General balance equation for a phase interface. *Ind. Engng Chem. Fund.* **6**, 108–115. (See also *Ind. Engng Chem. Fund.* **7**, 672.)

Slattery, J. C. 1972 *Momentum, energy, and mass transfer in continua*. McGraw-Hill.

Slattery, J. C. 1980 Interfacial transport phenomena. *Chem. Engng Commun.* **4**, 149–166.

Thomas, G. B. & Finney, R. L. 1980 *Calculus and analytic geometry*, p. 48. Addison-Wesley.

Tolman, R. C. 1948 Consideration of the Gibbs theory of surface tension. *J. chem. Phys.* **16**, 758–774.

Wasan, D. T., Gupta, L. & Vora, M. K. 1971 Interfacial shear viscosity and fluid-fluid interfaces. *A.I.Ch.E. Jl* **17**, 1287–1295.

Waxman, A. M. 1984 Dynamics of a couple-stress fluid membrane. *Stud. appl. Math.* **70**, 63–86.

Wei, L. Y. & Slattery, J. C. 1976 Experimental study of nonlinear surface stress-deformation behavior with the deep channel surface viscometer. In *Colloid and interface science* (ed. M. Kerker), vol. **4**, pp. 399–420. Academic.